NUREG/CR–5480
ORNL/TM–11399

Data Summary Report for Fission Product Release Test VI–3

Prepared by M. F. Osborne, R. A. Lorenz, J. L. Collins, J. R. Travis,
C. S. Webster, H. K. Lee, T. Nakamura, Y. -C. Tong

Oak Ridge National Laboratory

Prepared for
U.S. Nuclear Regulatory Commission

NUREG/CR--5480

TI90 012739

Data Summary Report for Fission Product Release Test VI–3

Manuscript Completed: May 1989
Date Published: June 1990

Prepared by
M. F. Osborne, R. A. Lorenz, J. L. Collins, J. R. Travis,
C. S. Webster, H. K. Lee, T. Nakamura, Y. -C. Tong

Oak Ridge National Laboratory
Operated by Martin Marietta Energy Systems, Inc.

Oak Ridge National Laboratory
Oak Ridge, TN 37831

Prepared for
Division of Systems Research
Office of Nuclear Regulatory Research
U.S. Nuclear Regulatory Commission
Washington, DC 20555
NRC FIN B0127
Under Contract No. DE–AC05–84OR21400

ABSTRACT

Test VI-3, the third in a series of high-temperature fission product release tests in the vertical test apparatus, was conducted in flowing steam. The test specimen was a 15.2-cm-long section of a fuel rod from the BR3 reactor in Belgium, which had been irradiated to a burnup of 42 MWd/kg. Using an induction furnace, it was heated under simulated light-water reactor (LWR) accident conditions to two test temperatures, 20 min at 2000 K and then 20 min at 2700 K, in a hot cell–mounted test apparatus. The released fission products were collected on components designed to facilitate sampling and analysis.

Posttest inspection confirmed that the cladding had been completely oxidized during the test. Only minimal fragmentation of the fuel specimen was found, however, and very little melting or fuel-cladding interaction had occurred. Based on fission product inventories measured in the fuel or calculated by ORIGEN2, analyses of test components showed total releases from the fuel of 100% for ^{85}Kr, 5% for ^{106}Ru, 99% for ^{125}Sb, and 99% for both ^{134}Cs and ^{137}Cs. A large fraction (27%) of the released ^{125}Sb was retained in the furnace, but most of the released cesium (89%) escaped to the collection system. Small release fractions for many other fission products were detected. In addition, very small amounts of fuel material – uranium and plutonium – were released. Including fission products and fuel and structural materials, the total mass released from the furnace to the collection system was 3.17 g, 78% of which was collected on the filters. The results from this test were compared with previous tests in this series and with a commonly used model for fission product release.

CONTENTS

FOREWORD

This document describes the ninth in a series of fission product release tests of commercial LWR fuel under severe accident conditions. Other reports describing the work conducted in this fission product release project are:

1. M. F. Osborne, R. A. Lorenz, J. R. Travis, and C. S. Webster, Data Summary Report for Fission Product Release Test HI-1, NUREG/CR-2928 (ORNL/TM-8500), December 1982.

2. M. F. Osborne, R. A. Lorenz, J. R. Travis, C. S. Webster, and K. S. Norwood, Data Summary Report for Fission Product Release Test HI-2, NUREG/CR-3171 (ORNL/TM-8667), February 1984.

3. M. F. Osborne, R. A. Lorenz, K. S. Norwood, J. R. Travis, and C. S Webster, Data Summary Report for Fission Product Release Test HI-3, NUREG/CR-3335 (ORNL/TM-8793), April 1984.

4. M. F. Osborne, J. L. Collins, R. A. Lorenz, K. S. Norwood, J. R. Travis, and C. S. Webster, Data Summary Report for Fission Product Release Test HI-4, NUREG/CR-3600 (ORNL/TM-9001), June 1984.

5. M. F. Osborne, J. L. Collins, R. A. Lorenz, K. S. Norwood, J. R. Travis, and C. S. Webster, Data Summary Report for Fission Product Release Test HI-5, NUREG/CR-4037 (ORNL/TM-9437), May 1985.

6. M. F. Osborne, J. L. Collins, R. A. Lorenz, K. S. Norwood, J. R. Travis, and C. S. Webster, Data Summary Report for Fission Product Release Test HI-6, NUREG/CR-4043 (ORNL/TM-9943), September 1984.

7. M. F. Osborne, J. L. Collins, R. A. Lorenz, J. R. Travis, and C. S. Webster, Design, Construction, and Testing of a 2000°C Furnace and Fission Product Collection System, NUREG/CR-3715 (ORNL/TM-9135), September 1984.

8. J. L. Collins, M. F. Osborne, R. A. Lorenz, K. S. Norwood, J. R. Travis, and C. S. Webster, Observed Behavior of Cesium, Iodine, and Tellurium in the ORNL Fission Product Release Program, NUREG/CR-3930 (ORNL/TM-9316), February 1985.

9. K. S. Norwood, An Assessment of Thermal Gradient Tube Results from the HI Series of Fission Product Release Tests, NUREG/CR-4105 (ORNL/TM-9506), March 1985.

10. M. F. Osborne, J. L. Collins, P. A. Haas, R. A. Lorenz, J. R. Travis, and C. S. Webster, Design and Final Safety Analysis Report for Vertical Furnace Fission Product Release Apparatus in Hot Cell B, Building 4501, NUREG/CR-4332 (ORNL/TM-9720), March 1986.

11. M. F. Osborne, J. L. Collins, and R. A. Lorenz, Highlights Report for Fission Product Release Tests of Simulated LWR Fuel, ORNL/NRC/LTR-85/1, February 1985.

12. M. F. Osborne, J. L. Collins, R. A. Lorenz, and T. Yamashita, Highlights Report for Fission Product Release Test VI-1, ORNL/NRC/LTR-86/7, March 1986.

13. M. F. Osborne, J. L. Collins, R. A. Lorenz, and T. Yamashita, Highlights Report for Fission Product Release Test VI-2, ORNL/NRC/LTR-86/18, December 1986.

14. M. F. Osborne, J. L. Collins, R. A. Lorenz, J. R. Travis, C. S. Webster, S. R. Daish, H. K. Lee, T. Nakamura, and Y.-C. Tong, Highlights Report for Fission Product Release Test VI-3, Draft Letter Report to SFD Partners, July 1987.

15. Toshiyuki Yamashita, Steam Oxidation of Zircaloy Cladding in the ORNL Fission Product Release Tests, NUREG/CR-4777 (ORNL/TM-10272), March 1988.

16. S. K. Wisbey, Preliminary Studies of the Morphology of Thermal Gradient Tube Deposits for Fission Product Release Experiments, NUREG/CR-4778 (ORNL/TM-10273), March 1988.

17. C. S. Webster and M. F. Osborne, The Use of Fiber Optics for Remote Temperature Measurement in Fission Product Release Tests, NUREG/CR-4721 (ORNL/TM-10366), April 1989.

18. M. F. Osborne, J. L. Collins, R. A. Lorenz, J. R. Travis, C. S. Webster, and T. Yamashita, Data Summary Report for Fission Product Release Test VI-1, NUREG/CR-5339 (ORNL/TM-11104), June 1989.

19. M. F. Osborne, J. L. Collins, R. A. Lorenz, J. R. Travis, and C. S. Webster, Data Summary Report for Fission Product Release Test VI-2, NUREG/CR-5340 (ORNL/TM-11105), September 1989.

20. M. F. Osborne and R. A. Lorenz, Fission Product Release at Severe Accident Conditions: FY 1989 Program Plan, ORNL/NRC/LTR-89/2, April 1989.

21. Takehiko Nakamura and R. A. Lorenz, Effective Diffusion Coefficients Calculated from ORNL Fission Product Release Test Results, NUREG/CR- (ORNL/TM-), in preparation.

ACKNOWLEDGMENTS

The authors gratefully acknowledge the significant contributions of several colleagues in conducting this work: C. W. Alexander for assistance with ORIGEN2 calculations of fission product inventories in the irradiated fuel; D. A. Costanzo and co-workers of the Analytical Chemistry Division for analyses of fission products, uranium, and plutonium; E. C. Beahm and T. B. Lindemer for technical consultation; Betty Drake for preparation of the manuscript; and C. S. Robinson for editing.

LIST OF FIGURES

LIST OF TABLES

DATA SUMMARY REPORT FOR FISSION PRODUCT RELEASE TEST VI-3

M. F. Osborne, R. A. Lorenz, J. L. Collins, J. R. Travis,
C. S. Webster, H. K. Lee, T. Nakamura, and Y.-C. Tong

1. EXECUTIVE SUMMARY

The objective of this report is to document as completely as possible the observations and results of fission product release test VI-3. Although all final data are not currently available, this report presents most of the results for potential use by other reactor safety researchers. Complete interpretation and correlation of these results with related experiments and with theoretical behavior will be included in a subsequent report, which will consider the results of several tests over a range of test conditions. Similar data summary reports for previous tests in this project, as well as other reports of related project activities, are listed in the Foreword.

The fuel specimen used in this test was cut from fuel rod I-1002, which was irradiated in the BR3 reactor in Belgium from July 15, 1976, to September 26, 1980. The fabrication and irradiation history of this fuel rod was compiled by Adams and Dabell. The fission product inventories, as measured in the fuel and calculated by ORIGEN2, and a description of the test procedure and conditions are included in Sect. 3. The test results and some preliminary interpretations are presented in Sect. 4, and these results are compared with data from previous tests in Sect. 5. The most important results are:

1. This was the highest-temperature test to date in the vertical induction furnace using three sequentially operated fission product collection trains and equipment for the continuous measurement of hydrogen. All of the experimental apparatus, including the ThO_2 furnace ceramics, performed quite well, and the test was considered entirely successful.

2. Posttest examination indicated that the Zircaloy cladding was completely oxidized, contained a number of minor fractures, and had experienced minimal melting or fuel-cladding interaction. The 15-cm-long specimen, however, did not collapse but remained in its original vertical orientation, although somewhat distorted.

3. The oxidation behavior of the Zircaloy cladding, as indicated by hydrogen generation, was in good agreement with tests VI-1 and VI-2 and with the Zircaloy oxidation model developed by Yamashita, using the generally accepted oxidation rates as functions of temperature.

4. The values for total release from the fuel specimen, based on gamma ray spectrometry measurements, were 100% for ^{85}Kr, 5% for ^{106}Ru, 99% for ^{125}Sb, and 99% for both ^{134}Cs and ^{137}Cs. About one-fourth of the released ^{125}Sb was deposited on the ThO_2 and ZrO_2

ceramics at the outlet end of the furnace, compared to almost complete transport of the released krypton and cesium from the furnace to the collection system. Pretest and posttest gamma ray spectrometry of the fuel was valuable in determining the release fractions as well as the axial distributions of the fission products along the fuel rod. Small amounts of other fission products - Rb, Mo, Tc, Pd, Ag, Te, Ba, and Eu - were detected in the collection system by other analytical techniques.

5. Small amounts of uranium and plutonium were found on the filters in all three trains of the test apparatus. Based on fluorimetric (chemical) analyses of leach solutions, 465 mg of uranium, which was about 0.69% of the fuel inventory, was collected on the filters. More than 99% of this amount was collected during the highest temperature part of the test, that is, in Trains B and C. The release fractions for plutonium were much lower, $\sim 10^{-4}$ of those for uranium. Data from two alternative methods of uranium analysis showed that inductively coupled plasma-emission spectrometry (ICP-ES) results agreed well with the fluorimetric results, but that the less precise spark source mass spectrometry (SSMS) results tended to be about a factor of two higher.

6. The fission product distributions in the thermal gradient tubes (TGTs) showed a very high concentration of cesium near the entrance of TGT B, at a deposition temperature of ~975 K (~700°C). The most probable composition of this material was concluded to be $CsMoO_4$. Smaller peaks of cesium and of antimony were found at similar locations in the TGTs of both Trains B and C. Comparable behavior of cesium and antimony has been observed in previous tests.

7. The total masses of deposits on the TGTs and filters were determined by direct weighing to be 3.17 g, with 78% of this (2.49 g) being deposited on the filters. As would be expected, the mass release rates were highest during the highest-temperature period of the test. The maximum aerosol concentration, averaged over the collection period, was 15 g/m^3 at 423 K (150°C) during test Phase B.

8. Comparison of the release data from this test with the results of previous tests provided evidence that the CORSOR-M model over-predicts the release of volatile fission products by factors of 3 to 10 in the temperature range of 2300 to 2700 K.

2. INTRODUCTION

This report summarizes data from the third test in a vertical test apparatus. This series of tests is designed to investigate fission product release from light-water reactor (LWR) fuel in steam and/or hydrogen in the temperature range of 2000 to 2700 K. Earlier tests, conducted under similar conditions at temperatures of 773 to 1873 K (500

to 1600°C), were reported in detail by Lorenz et al.;[1-4] additional tests at higher temperatures (~1700 to 2300 K) were reported by Osborne et al.[5-12] The purpose of this work, which is sponsored by the U.S. Nuclear Regulatory Commission (NRC), is to obtain the experimental data needed to reliably assess the consequences of a variety of heatup accidents in LWRs.* The specific objectives of this program are:

1. to obtain fission product release and behavior data applicable to the analysis of reactor accidents, and

2. to apply these data to the development of VICTORIA and other release and transport models.

Tests of high-burnup LWR fuel are emphasized in this program. The applicability of simulated fuel (unirradiated UO_2 containing radioactive fission product tracers) has been considered, and several simulant tests have been conducted to provide valuable data about the behavior of specific fission product species.[13,14] All tests have been conducted at atmospheric pressure in a flowing mixture of steam and helium in a hot cell. Steam concentrations have been varied to simulate different accident sequences or core locations.

The procedures and techniques used in preparing and conducting the test, as well as in posttest examination and analysis, were very similar to those used for the six tests in the HI series[5-10] and in tests VI-1 and VI-2.[11,12] The analytical techniques employed are listed in Table 1. This report provides a brief description of test VI-3 and a tabulation of all the results obtained to date. Because some of the analyses have been delayed and the results will not be available for several months, they will be published together with similar results in a later report. Thorough data evaluation and correlation of all results from the VI test series will be included in subsequent reviews and reports covering this series of fission product release tests at temperatures up to 2700 K.

3. TEST DESCRIPTION

The vertical test apparatus is operated remotely and is capable of conducting tests at temperatures up to 2700 K for time periods up to 60 min in reactive atmospheres of steam and/or hydrogen mixed with helium.[15] Details of the furnace are shown in Fig. 1, and the entire test apparatus is illustrated in Fig. 2. Good measurement and control of temperature and gas flow rates have been demonstrated. Both manual and automatic optical pyrometers are used for temperature measurement, supplemented by thermocouples during the low-temperature heatup phase. The released fission products are collected in three sequentially operated, parallel collection trains, each composed of a platinum or

---

*M. F. Osborne, R. A. Lorenz, and R. P. Wichner, "Program Plan for Fission Product Release from LWR Fuel in Steam," memorandum to USNRC, April 1982.

Table 1. Analytical techniques for fission product analysis

Technique	Time	Location	Elements
Gamma spectrometry	Pretest, posttest	Fuel specimen	Long-lived, gamma-emitting fission products - Ru, Ag, Sb, Cs, Ce, Eu
	On-line	Thermal gradient tube (TGT), charcoal traps, filters	Cs, Kr
	Posttest	Furnace components, TGT, filters	Ru, Ag, Sb, Cs, Ce, Eu
Neutron activation analysis	Posttest	Charcoal, solution from furnace, TGT, filters	I, Br, (Te, Mo, Ba)[a]
Chemical analysis	Posttest	Furnace, filters	U, Pu
Spark-source mass spectrometry	Posttest	Samples from furnace, TGT, filters	All elements with atomic numbers ≥10
Inductively coupled plasma-emission spectrometry	Posttest	Acid solutions from furnace, TGT, or filters	Many cations, especially Mo, Te, Ba, U
Scanning electron microscope with energy dispersive X-ray system	Posttest	TGT, aerosol sampler	All elements with atomic numbers ≥10

[a]Iodine and bromine have been analyzed by neutron activation throughout HI and VI test series; neutron activation analysis techniques for Te, Mo, and Ba are in various stages of development.

ORNL DWG 85-496R2

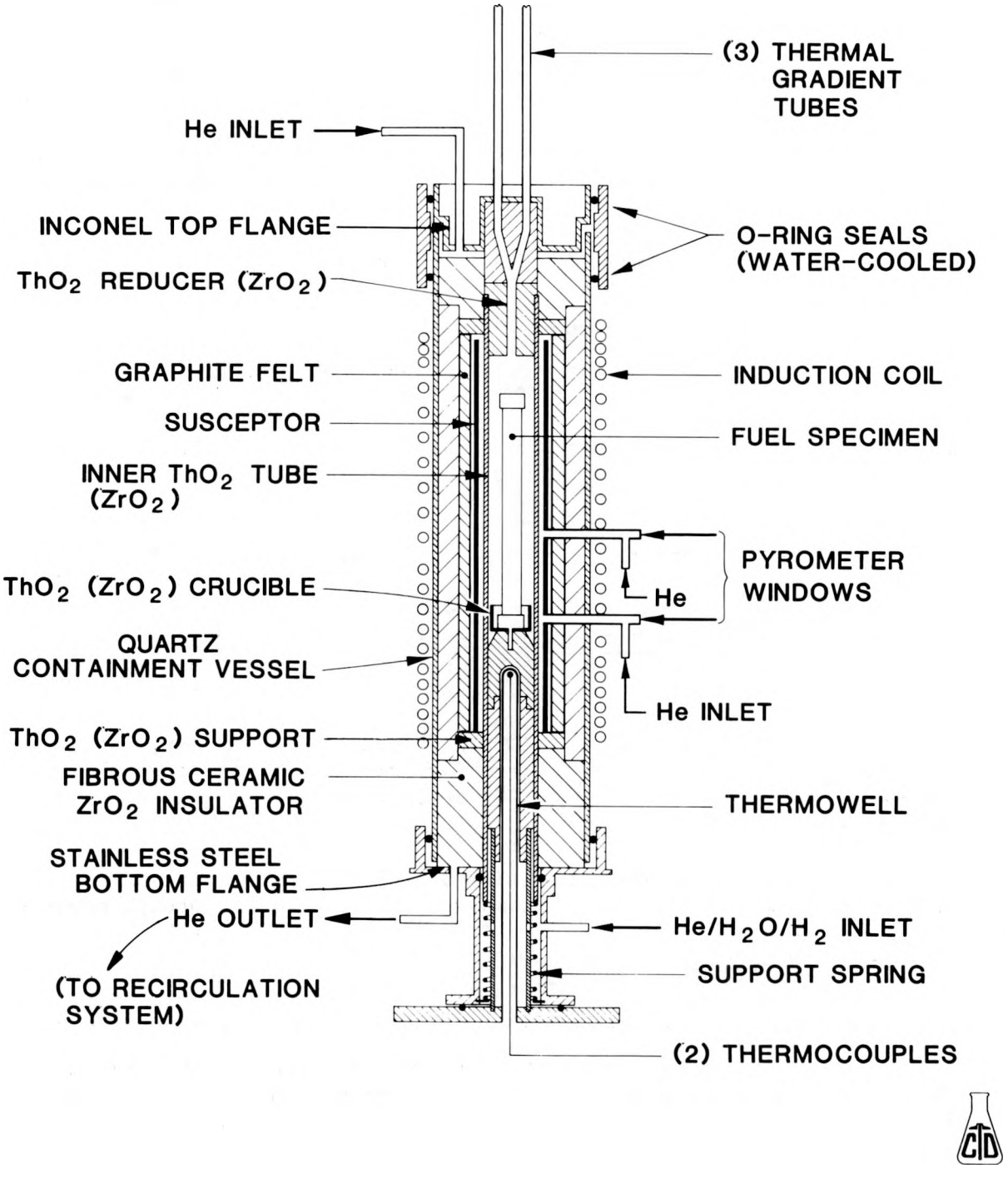

Fig. 1. Vertical induction furnace for fission product release tests.

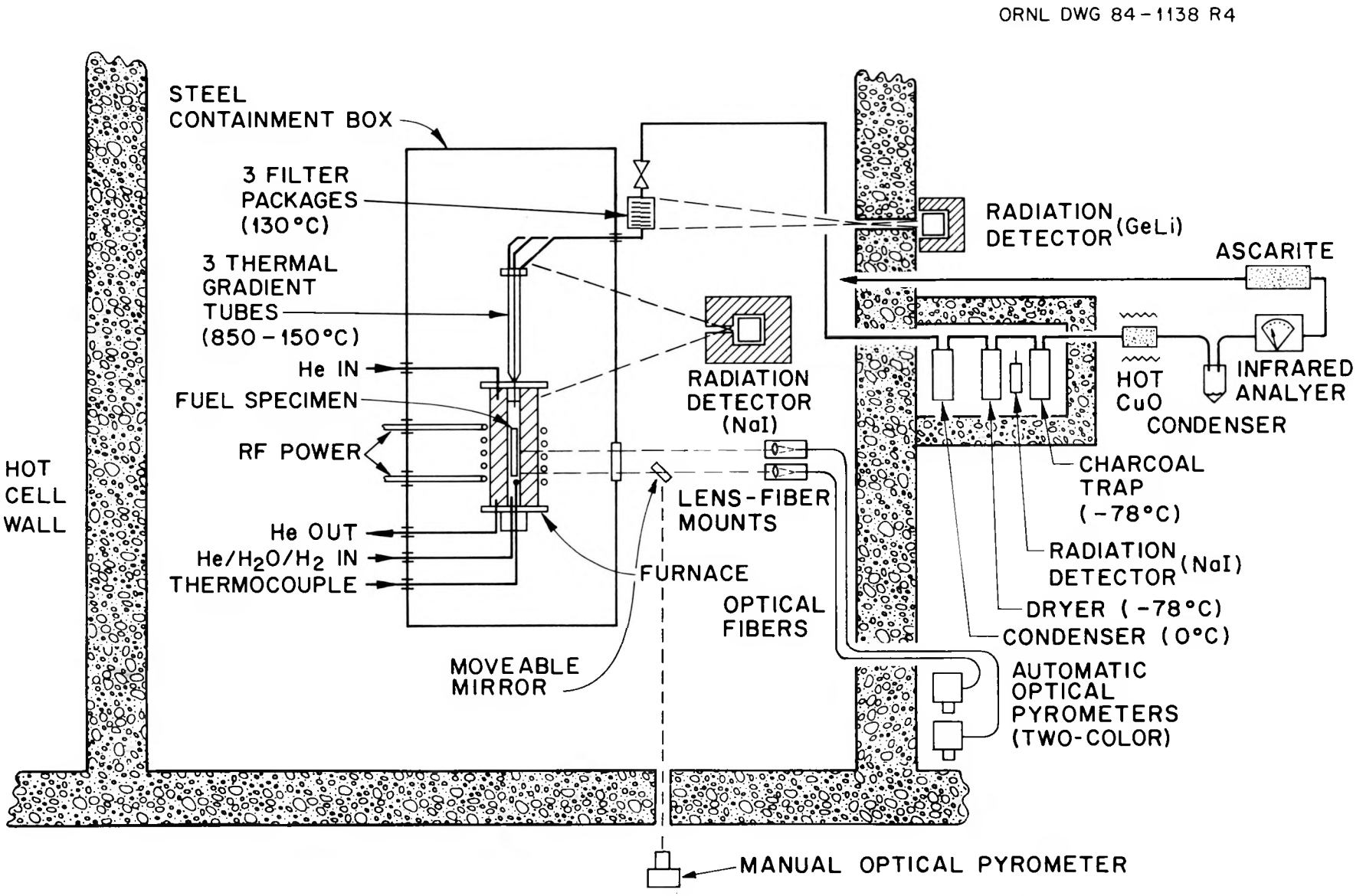

Fig. 2. Vertical fission product release test apparatus.

stainless steel-lined TGT, a filter package containing graduated fiberglass filters and heated charcoal for iodine sorption, and cold charcoal traps for rare gas collection. The on-line releases of ^{85}Kr and ^{137}Cs are monitored by detectors observing these components. The effluent gases pass through a hot CuO bed where the hydrogen generated by reaction of steam with the Zircaloy cladding is converted to water. The collection of this water in a condenser is measured continuously by a modified conductivity meter, thereby enabling determination of the oxidation rate of the cladding. Details of the fission product collection system are shown in Fig. 3.

The tests planned for this vertical apparatus assume that temperature (2000 to 2700 K) is the dominant variable. Steam flow rate (0.3 to 1.5 L/min) and time (1 to 60 min), both of which affect the extent of oxidation, are secondary variables. The objectives of this particular test were twofold: (1) to obtain release data from BR3 fuel at 2000 K for a period of 20 min (Phase A) in steam flowing at a high rate for comparison with results from Phase A of test VI-1, and (2) to determine the release and fuel behavior during a subsequent heatup and 20 min period at 2700 K, the highest test temperature to date in this project.

3.1 FUEL SPECIMEN DATA

The test specimen was a 15.2-cm-long section of rod I-1002 from the BR3 reactor in Belgium, as shown in Fig. 4. This fuel was irradiated from July 15, 1976, until September 26, 1980. Details of the irradiation and of the characteristics of this particular specimen were reported by Adams and Dabell* and are listed in Table 2. The fuel in this rod had an initial enrichment of 5.76% ^{235}U, and the VI-3 specimen had attained a burnup of ~42 MWd/kg during irradiation. Fission product inventories for the specimen were measured by direct gamma spectrometry of the fuel and/or were calculated with the ORIGEN2 computer program,[16] with adjustments based on direct analyses for ^{137}Cs in the fuel; these data are shown in Tables 3 and 4.

No axial scan of the gamma radioactivity along the intact fuel rod was made before the rod was sectioned. Scans of nearby rods with similar operating histories, however, indicated that rod I-1002 contained no unusual distributions of fission products and that the operating power was not high enough to cause migration of such volatile fission products as cesium. Although no gas analyses were obtained for rod I-1002, examination of these data from comparable rods and our thin-slit gamma scan data for this specimen indicated that the release of ^{85}Kr from the fuel in the region of the test specimen was 10%. Reactor operating data indicated that this fuel rod had operated at a maximum linear power of 251 W/cm averaged over the 1 m length.* The fuel in the peak burnup region (near midlength) would have operated at a peak

---

*J. P. Adams and B. R. Dabell, "Characteristics of UO_2-Zr Fuel Rods Irradiated in the BR3 Reactor," private communication, 1986.

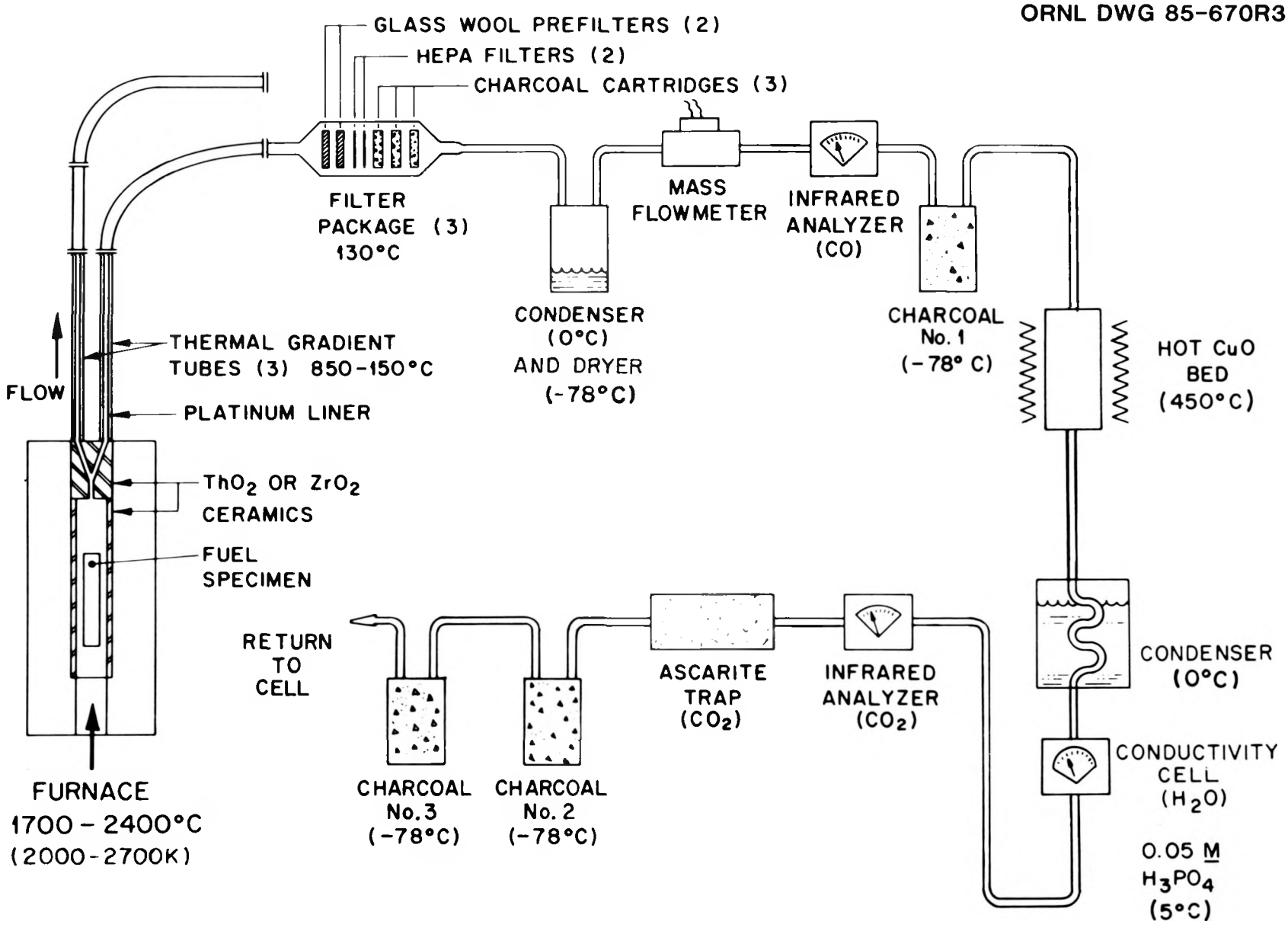

Fig. 3. Components of fission product collection system.

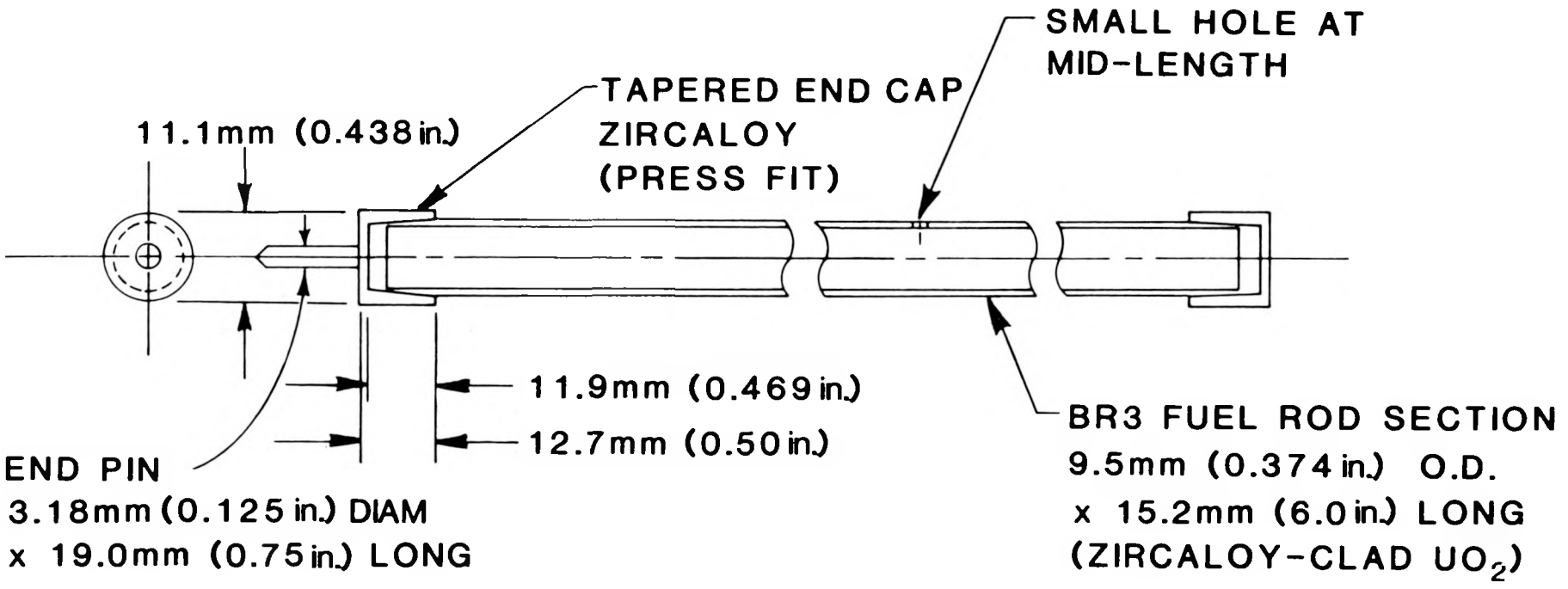

Fig. 4. Details of fuel specimen in test VI-3.

Table 2. Fuel, temperature, and flow data for test VI-3

Parameter	Value
Fuel specimen:	
Length	15.2 cm
Mass UO_2	81.1 g
Mass Zircaloy	21.2 g
Burnup	42 MWd/kg
Kr in-pile release	10%
Specimen temperature:	
At start of heatup ramp	~500 K
Heatup rate	~0.3 K/s
Test temperatures	2000, 2700 K
Times at test temperature	20, 20 min
Time >2000 K	90 min
Cooldown rate (controlled)	~0.5 K/s
Gas flow rates:	
Helium into furnace	0.6 L/min[a]
Steam into furnace	~1.6 L/min (~1.2 g/min)
Helium within recirculation system	~1.5 L/min
Effluent collected:	
Steam in condenser and dryer	222.9 g

[a]L = liter at standard temperature and pressure.

Table 3. Inventories of principal fission product elements in test VI-3 fuel[a]

Elements	Amounts in fuel (g/MTU)	Amounts in test specimen[b] (mg)
Se	75.99	5.435
Br	29.20	2.088
Kr	513.4	36.72
Rb	505.6	36.16
Sr	1,171	83.75
Y	667.0	47.70
Zr	4,959	354.7
Mo	4,322	309.1
Tc	1,001	71.59
Ru	2,544	181.9
Rh	535.7	38.31
Pd	1,230	87.97
Ag	61.63	4.408
Cd	87.26	6.241
In	2.56	0.183
Sn	88.86	6.355
Sb	20.82	1.489
Te	557.4	39.87
I	261.2	18.68
Xe	6,611	472.8
Cs	3,240	231.7
Ba	2,126	152.1
La	1,589	113.6
Ce	3,111	222.5
Eu	152.0	10.87
Total fission products	43,430	3,106
U	947,400	67,760
Pu	8,157	583.4
Total actinides	956,600	68,420

[a]Inventories for this BR3 fuel were calculated by ORIGEN2, assuming a burnup of 42,000 MWd/MTU, and were corrected for decay to July 1, 1986.

[b]The test VI-3 specimen contained 71.52 g U (81.13 g UO_2), which is equal to 7.152E-05 MTU before irradiation.

Table 4. Inventory of long-lived radionuclides in test VI-3 fuel[a]

Radionuclides	Amounts in fuel (g/MTU)	Amounts in fuel (Ci/MTU)	Amounts in test specimen[b] (mg)	Amounts in test specimen[b] (mCi)
		Fission products		
^{85}Kr	21.79	8,551	1.558	611
^{90}Sr	661.60	90,290	47.32	6,458
^{106}Ru	1.79	5,995	0.128	428.8
^{110m}Ag	0.0013	6.32	0.00010	0.452
^{125}Sb	2.58	2,669	0.185	190.9
^{129}I	203.30	0.036	14.54	0.0026
^{134}Cs	16.08	20,810	1.150	1,488
^{137}Cs	1,292.00	112,400	92.40	8,039
^{144}Ce	1.64	5,246	0.118	375.2
^{154}Eu	24.62	6,650	1.761	475.6
Total fission products	43,430.00	499,000	3,106	35,690
		Actinide elements		
^{234}U	302.8	1.893	21.66	0.135
^{235}U	17,830	0.03856	1,275.00	0.003
^{236}U	6,989	0.4523	499.90	0.032
^{238}U	922,300	0.3102	65,960.00	0.022
Total U	947,400	4.598	67,760.00	0.329
^{238}Pu	160.9	2,756	11.51	197.1
^{239}Pu	4,858	302.1	347.4	21.61
^{240}Pu	2,117	482.5	151.4	34.51
^{241}Pu	739.9	76,260	52.92	5,454
^{242}Pu	281.1	1.074	20.10	0.077
Total Pu	8,157	79,800	583.40	5,707
Total actinides	956,600	81,460	68,420	5,826

[a]Inventories for this BR3 fuel were calculated by ORIGEN2, assuming 42,000 MWd/MTU, and were corrected for decay to July 1, 1986. The values used to calculate the releases of ^{125}Sb (102.6 mCi) and ^{137}Cs (8.770 Ci) were measured by gamma spectrometry.

[b]The test VI-3 specimen contained 71.52 g U, which is equal to 7.152E-05 MTU before irradiation.

linear power of >300 W/cm at that time. The data used to estimate fission gas release from the peak burnup region of a fuel rod are shown in Fig. 5. Using Fig. 5 and the operating history, we estimate that ~10% of the total krypton generated in the fuel had been released during irradiation. The conversion from average gas release to release from the peak power (and burnup) location was made using the D' (empirical) method.[17]

In addition to the test VI-3 fuel specimen, three other 15.2-cm-long specimens were cut from rod I-1002 and prepared for future testing. One of these adjacent sections was heated previously in test VI-2.[12] Three short samples (1 to 2 cm long) were cut for metallographic examination, for dissolution and chemical analysis, and as an archive sample for possible future use.

Tapered end caps of Zircaloy-2 were pressed onto the ends of the test specimen, not as gas seals, but to prevent loss of the fractured UO_2 fuel during subsequent handling. The bottom end cap included a pin to facilitate vertical mounting. A small hole, 1.6 mm in diameter, was drilled through the cladding at midlength to serve as a standard leak for gas release during the heatup phase of the test. These details are shown in Fig. 4.

3.2 TEST CONDITIONS AND OPERATION

As in each of the previous experiments, the test apparatus was assembled by direct handling, which is possible because the hot cell and test apparatus are decontaminated after each test. Also, new furnace internals, TGT liners, and filter package components are used in each test. Only the transfer and loading of the highly radioactive fuel specimen and the final closure of the furnace and containment box were done remotely. No in-cell operations were required during the test. Before heating and steam flow were begun, the test apparatus was evacuated and purged with helium. All connecting lines to the furnace, TGT, and filter assemblies were preheated to at least 125°C to prevent steam condensation during the test.

This test was intended to investigate fission product release at two temperatures (2000 and 2700 K) under strongly oxidizing conditions. The operating conditions are summarized in Table 2, and the temperature history is shown in Fig. 6. In tests VI-1 and VI-2, which used all ZrO_2 furnace ceramics, heatup rates of ~1 K/s were used. At the higher temperature of this test (2700 K), however, a ThO_2 furnace tube was required. Because of the greater susceptibility of ThO_2 to thermal shock, a slower heatup rate (~0.3 K/s) was necessary in test VI-3.

The most important events during the test are listed in the test chronology, Table 5. The time periods for operation of the three collection trains (Fig. 6) were for Train A, 0 to 106 min; for Train B, 106 to 138.5 min; and for Train C, 138.5 min to end of test, including cooldown. A preheat period was included to slowly heat the specimen to

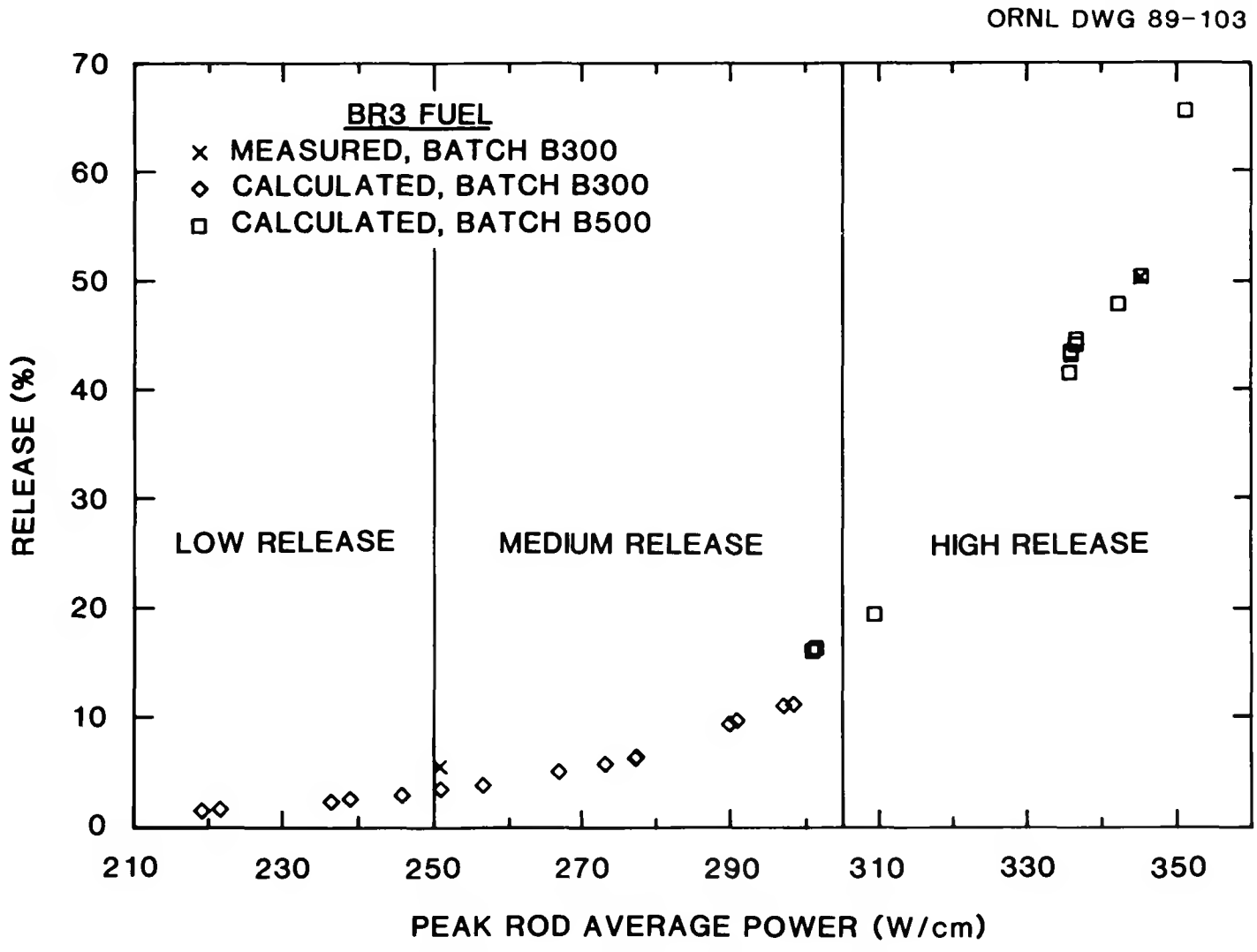

Fig. 5. In-reactor release of volatile fission products as a function of average power. Note rapid increase in release above 300 W/cm.

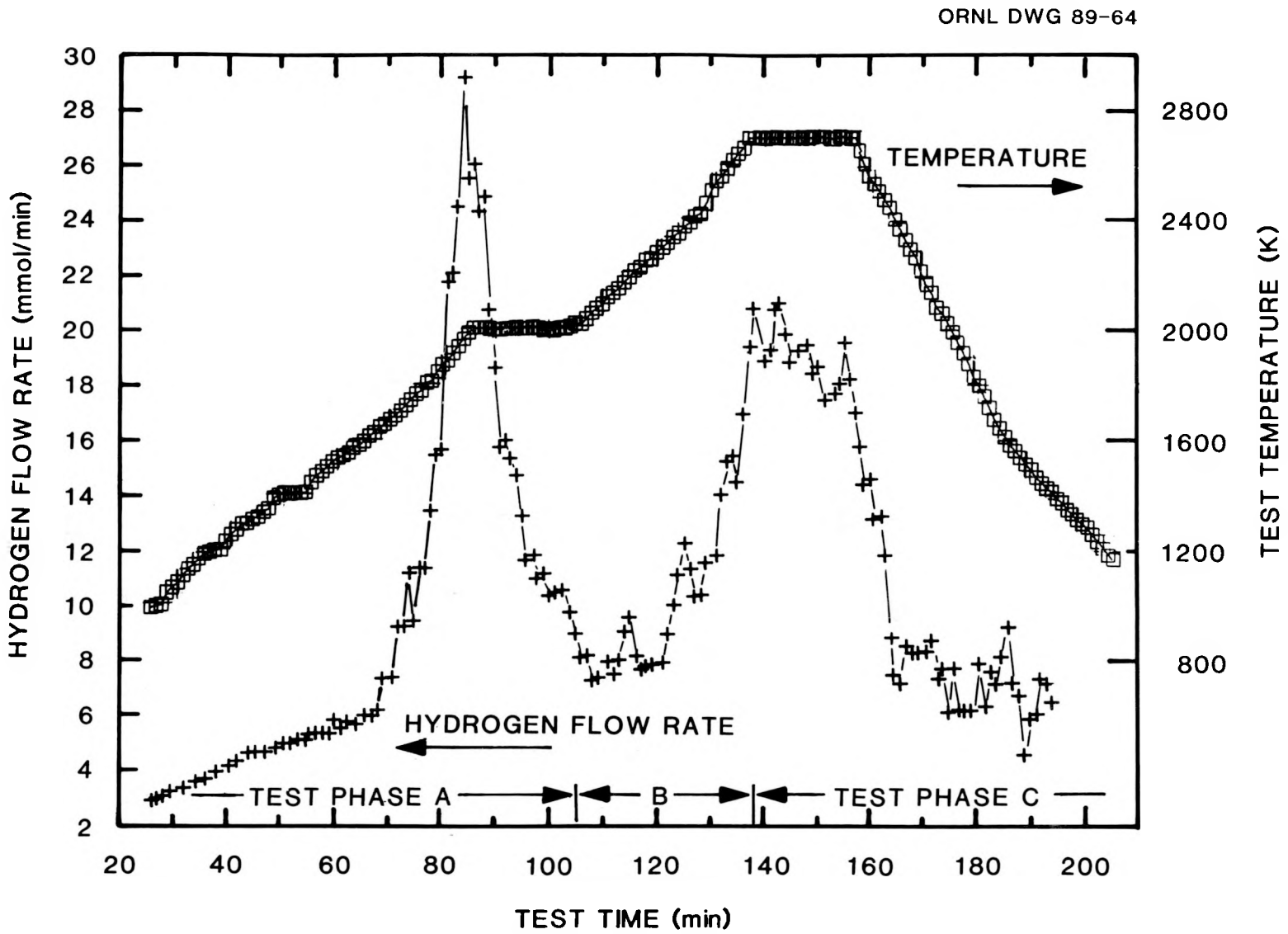

Fig. 6. Temperature and hydrogen production history in test VI-3.

Table 5. Chronology of test VI-3, April 8, 1987

Event/status	Time		Corrected furnace temperature[a] (K)
	Clock	Test	
Load fuel into furnace	900		Room temperature
Heat steam system	1000		Room temperature
Problems with TR-2, CuO beds, etc.	1100		Room temperature
Begin furnace preheat	1312		~350
Begin steam flow to furnace	1335		~500
Thermal gradient tube (TGT) to 750°C to oxidize stainless steel TGT	1342		~515
Reduce power to TGT	1407		
Test phase A			
Start ramp	1440	0	~500
First micro measurement	1505	25	984
Reached 1400 K	1530	50	1404
Resumed ramp	1534	54	1406
Reached 2000 K	1606	86	2003
Increased TGT power	1608	88	2002
Test phase B			
Switch to train B, resume ramp	1626	106	2008
Last Pt-Rh thermocouple measurement (1718°C)	1645	125	2367
Reached 2700 K	1657	137	2698
Test phase C			
Switched to train C	1658:30	138.5	2700
End 2700 K phase, reduce power	1717	157	2708
Down to 2000 K	1736	176	1995
Down to 1400 K	1755	195	1414
Last IRCON measurement	1800	200	1315
Last micro measurement, furnace off	1810	210	1068
Reduce power to TGT, cool down	1812	212	

[a]Readings by manual optical pyrometer, corrected for emissivity and losses through windows. Low temperatures were estimated from thermocouple at furnace entrance.

550 K prior to beginning steam flow to the furnace. Time zero was defined as that time when the controlled heating ramp was begun, with stable steam flow through the warm furnace established. Temperature measurement and control were generally good. The 8-min period at 1400 K was included to ensure heatup of ceramics in the outlet end of the furnace and to compare the data from the three optical pyrometers before any significant release of fission products had occurred. The calculated hydrogen production history, using the model of Yamashita,[18] is shown in Fig. 7. This model indicates that the Zircaloy cladding should have become oxidized within 1 min after reaching 2000 K, which agrees well with the experimental data in Fig. 6.

3.3 POSTTEST DISASSEMBLY AND EXAMINATION

After the test was completed, the apparatus was monitored for the distribution of radioactivity and then disassembled. Initially, the filter assemblies and the TGT liners were removed and transferred to another hot cell to avoid potential contamination from fuel handling. The top flange was removed from the furnace, and after removal of the ceramic components from the outlet end, the top end of the fuel specimen could be observed. To preserve the geometry of the fuel for sectioning and subsequent microstructural examination, the furnace tube was filled with epoxy resin.

4. TEST RESULTS

4.1 TEST OBSERVATIONS

The test was conducted as planned and no unusual events or problems arose. Upon removal of the top flange and the ceramics at the outlet end of the furnace, the top end of the fuel specimen was visible. Although apparently heavily oxidized, the Zircaloy end cap was visible, and the top end of the specimen had tilted to make contact with the ThO_2 furnace tube (see Fig. 8). The fact that the specimen remained largely intact and upright after the very high temperature test was somewhat surprising. The furnace test zone was slowly filled with epoxy resin to ensure retention of fuel specimen geometry and to minimize the spread of radioactive material during handling. The furnace tube–fuel specimen assembly was then removed to another hot cell. After inspection and detailed gamma scanning, it was subsequently transferred to Sandia National Laboratories (SNL), where it was inspected by X ray in conjunction with examination of SNL tests ST-1 and ST-2. Following this work, the specimen was transferred to Argonne National Laboratory (ANL) for sectioning and detailed examination of cross sections.

4.2 TEST DATA

Test temperature and the hydrogen production rate are plotted as a function of test time in Fig. 6. In agreement with test VI-1,[11] the hydrogen production rate curve in Fig. 6 indicates a peak at the time the fuel reached about 2000 K, then a decline as most of the Zircaloy

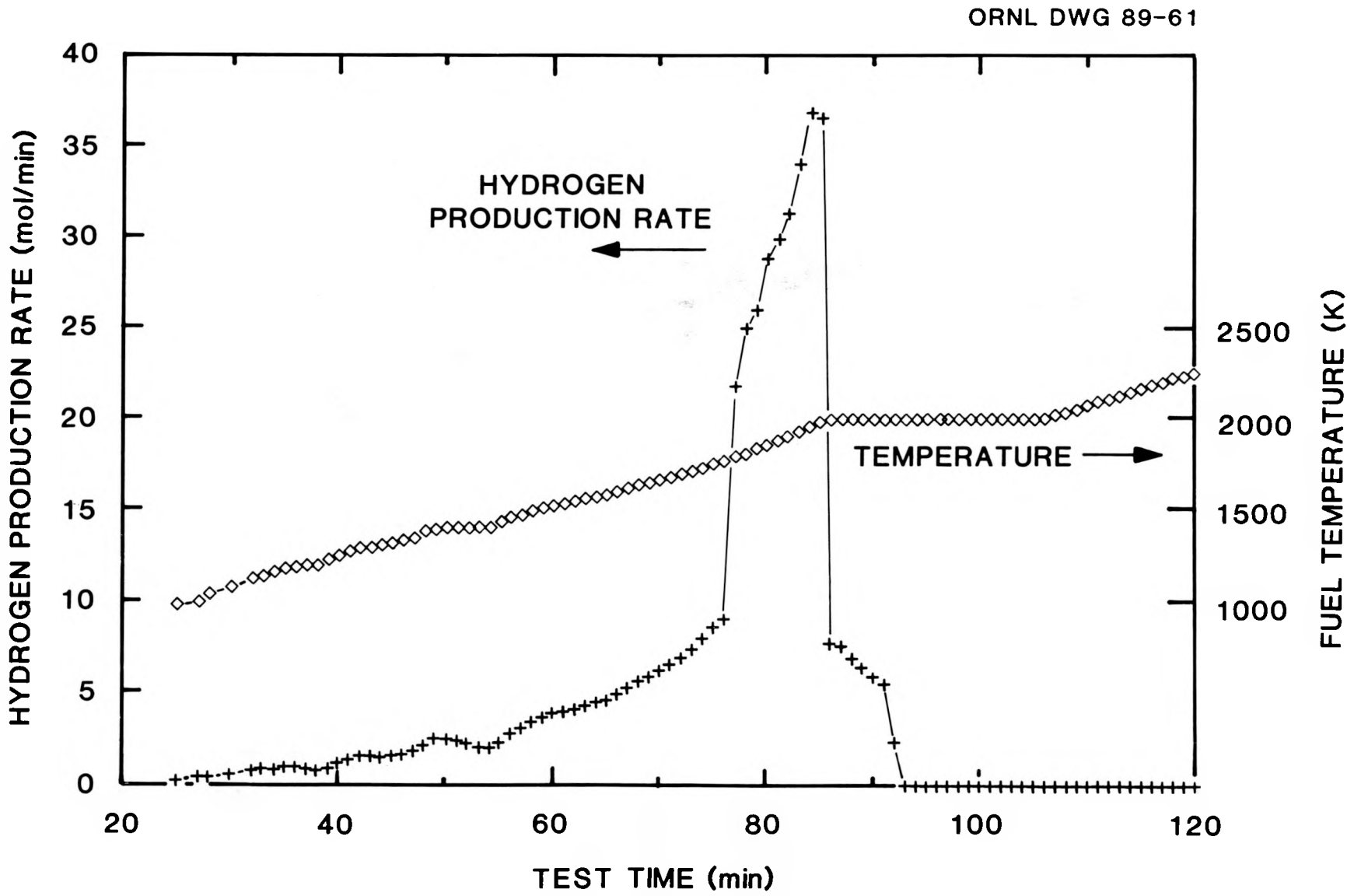

Fig. 7. Calculated hydrogen production history as functions of time and temperature.

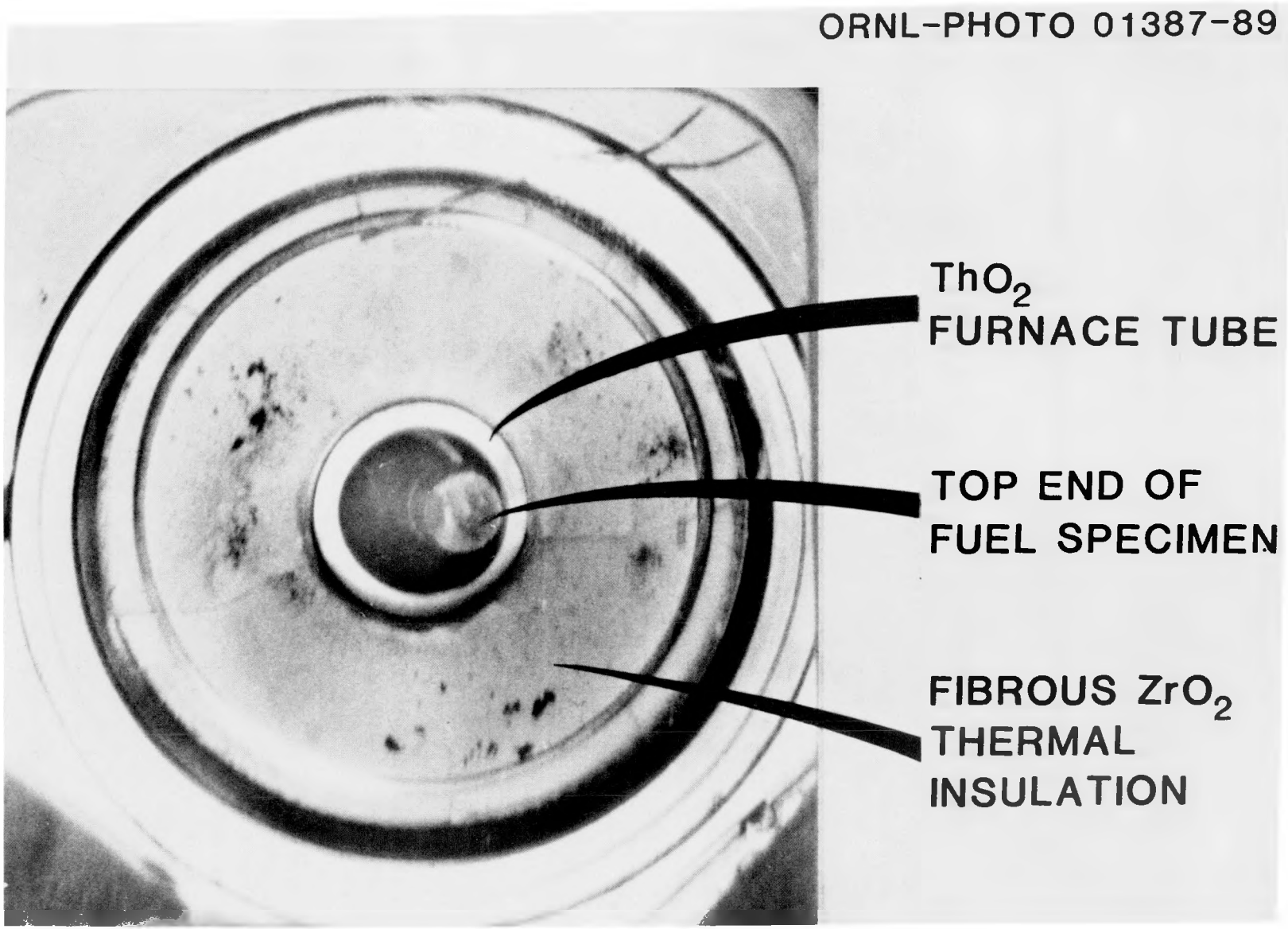

Fig. 8. Top view of furnace, showing top end of fuel specimen, after test VI-3.

cladding became fully oxidized to ZrO_2. The second, somewhat lower peak during the 2700 K phase (137 to 157 min) probably indicates oxidation of (1) the thicker Zircaloy end caps, (2) the graphite susceptor by steam leaking into the heater region, and/or (3) possibly the UO_2. This cladding oxidation behavior correlated well with the model developed by Yamashita.[18] This model incorporated the oxidation rate coefficients of both Baker and Just[19] and Urbanic and Heidrick[20] as well as the specific geometry and temperature of our test in order to calculate the progressive oxidation of the cladding during the test.

4.3 POSTTEST DATA

4.3.1 Gamma Spectrometry

Using Ge(Li) detectors and standard gamma spectrometry procedures, all experimental components and collectors were analyzed after the test under well-defined geometry to determine the concentration of the gamma-emitting fission products. In addition, the techniques that were developed for processing the release data for test VI-1 were used to provide more precise results.[11] Because all samples required at least double containment (metal, glass, or plastic) and because many samples were actually distributed within other materials (especially the fuel specimen itself), it was difficult to calculate accurately the effective shielding for the various gamma-ray energies of interest. Considering the ubiquitous nature of cesium and the broad range of gamma-ray energies inherent to ^{134}Cs (475 to 1365 KeV), an empirical method of determining the effective shielding to obtain a mass balance for cesium among several of the ^{134}Cs gamma-ray energies was developed. This shielding value was then applied to other nuclides, such as ^{106}Ru, ^{110m}Ag, and ^{125}Sb, to provide more accurate results.

Pretest gamma spectrometric analysis of the 15.2-cm-long fuel specimen was used to determine the fission product inventories in the fuel. Long-lived gamma emitters – ^{106}Ru, ^{125}Sb, ^{134}Cs, ^{137}Cs, ^{144}Ce, and ^{154}Eu – were determined directly. A calculation by the computer program ORIGEN2, with corrections based on ^{137}Cs data, supplied the inventory values for other fission products, activation products, and fuel nuclides, as shown in Tables 3 and 4. The axial distributions of the gamma-emitting fission products measured in the fuel before the test are shown in Fig. 9. These pretest data, based on measurements at 2-cm intervals, showed that the distributions of these major fission products were relatively uniform along the rod. Consequently, we conclude that (1) the burnup was similarly uniform, and (2) the operating temperature was not high enough to cause significant migration of volatile species such as cesium. The detailed posttest gamma scan of the fuel specimen, obtained with a 0.05-cm collimator, is shown in Fig. 10. The gaps between fuel pellets appear clearly in both the gamma scan and the adjacent X-ray view supplied by SNL. This X-ray view also shows the intact, but somewhat distorted, shape of the specimen.

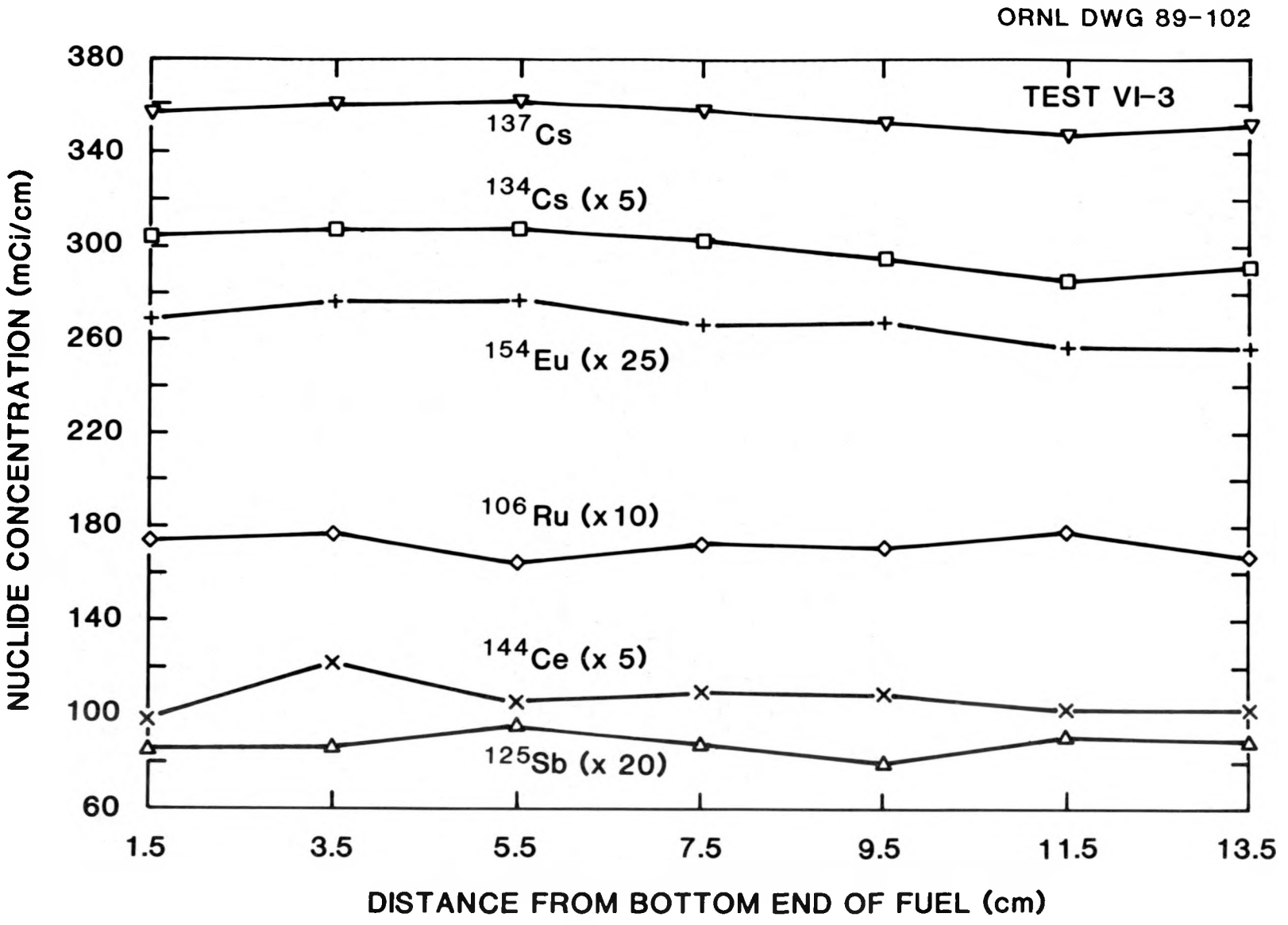

Fig. 9. Relative distributions of major fission products in fuel specimen before test VI-3.

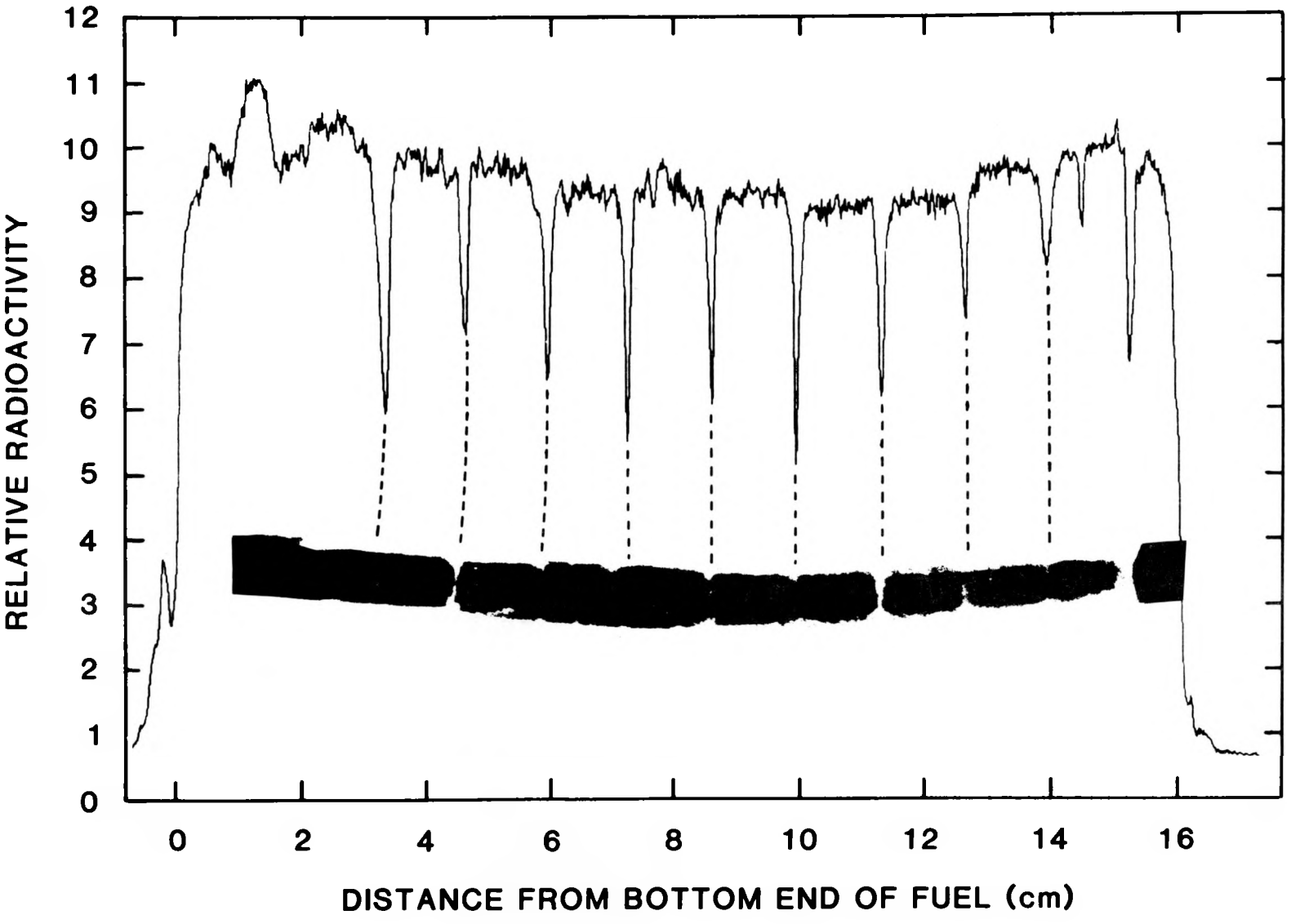

Fig. 10. Posttest gamma ray profile and X-ray view of test VI-3 fuel specimen.

As has been typical of these tests of high-burnup, long-decayed fuel, ^{137}Cs and ^{134}Cs were the dominant activities in almost all samples and interfered with the analysis of less abundant fission products. The release behaviors of krypton and cesium as functions of time and temperature are illustrated in Fig. 11; these curves show that most of the release occurred early in the high-temperature period, leaving very little volatile material available for release during the last half of the high-temperature period. On-line analysis indicated that the krypton release value reached about 100% by the end of test phase B. (An estimated 10% of the krypton inventory was released from the UO_2 to the pellet-cladding gap during irradiation and had been released when the rod was sectioned.)

A summary of the fractional release results for Kr, Ru, Sb, and Cs, as determined by gamma spectrometry, and also for U is presented in Table 6. Although no data for ^{134}Cs are shown, the agreement with ^{137}Cs was consistently good at all locations. The distribution of cesium within the test apparatus is shown in detail in Table 7. As has been noted previously, the largest fraction of the cesium (58%) was released during Phase B, the 31-min heatup period from 2000 to 2700 K and the 1.5-min period at 2700 K. Much smaller amounts of cesium were collected during Phases A and C (~19 and 11% respectively). About 11% of the released cesium was retained in the furnace. As usual, the cesium fractions collected on the filters were much larger than the fractions collected in the TGTs, an indication that the majority of the cesium was associated with the aerosol (either as particles or deposited on other particles) rather than being transported as vapor. No release data for iodine are available at this time; these data will be reported later.

The indicated release values for ^{106}Ru and ^{125}Sb are shown in Table 8. Although these nuclides are of relatively low yield and are not among the most hazardous, they have intermediate half-lives and strong gamma rays, which make them easily detected. The releases of antimony (98.8%) and ruthenium (5.0%) appear to have been higher than in any previous test, apparently a result of the very high test temperature. In several previous tests, significant release fractions for ^{110m}Ag were measured. In this test, however, the data for silver were quite sparse; this is partially a result of the longer decay time and correspondingly lower decay rates for the BR3 fuel in this test (~7 years). A second, and perhaps more important, reason for this failure to measure ^{110m}Ag in test VI-3 is a change in components used in the multichannel analyzer system. This change resulted in a small reduction in resolution of the gamma ray energies, thereby reducing the capability to measure marginal radionuclides, such as ^{110m}Ag. As shown in Table 8, large fractions (88% and 27% respectively) of the released Ru and Sb were deposited on ceramic surfaces in the outlet region of the furnace, where temperatures were believed to be 1300-1800 K during the test.

The relative posttest distributions of the fission products ^{106}Ru, ^{137}Cs, ^{144}Ce, and ^{154}Eu in the fuel specimen are shown in Fig. 12. The

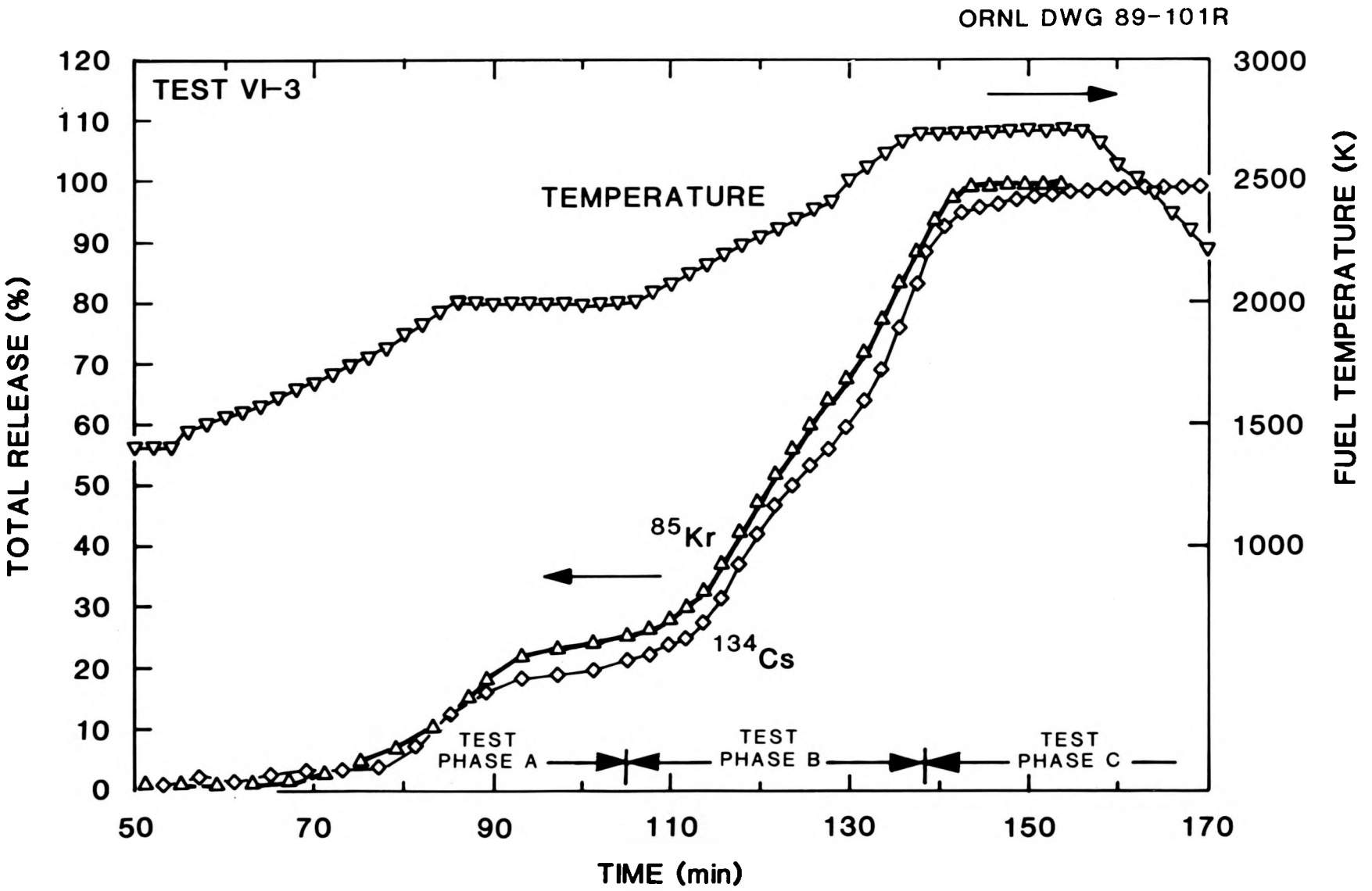

Fig. 11. Temperature, fission product release, and collection train operating histories for test VI-3.

Table 6. Summary of release data for test VI-3

Component/ collector	Operating time T >2000 K (min)	Percentage of fission product inventory[a] found				
		^{85}Kr	^{106}Ru	^{125}Sb	^{137}Cs	U
Furnace	90	0	4.43	26.25	23.59	10.48
Train A	20					
TGT			0	0	3.20	
Filters			0	0	15.97	0.00046
Total		0	0	0	19.18	
Train B	32.5					
TGT			0	13.30	16.14	
Filters			0.02	45.55	42.27	0.247
Total		0	0.02	58.85	58.42	
Train C	37.5					
TGT			0	4.08	3.14	
Filters			0.57	9.50	7.63	0.440
Total		0	0.57	13.58	10.77	
Cold charcoal, condenser, etc.	90	100[b]	0	0	0.004	
Total for test	90	100[b]	5.01	98.68	98.84	0.687

[a]Inventories based on pretest fuel analysis and ORIGEN2 calculations.

[b]An estimated 10% of the ^{85}Kr was released during irradiation; apparently, all of the remaining ^{85}Kr was released during test.

Table 7. Cesium release and distribution data for test VI-3[a]

Location	Approximate temperature (K)	Cesium found at each location			
		^{137}Cs (mCi)	Total Cs (mg)	Percent of inventory	Percent of released
Furnace components					
Inlet parts	500–1800	0.163	0.005	0.002	0.00
ThO_2 plug	~2500	8.04	0.232	0.092	0.09
ZrO_2 plug	~2000	769.0	22.16	8.769	8.87
ZrO_2 donut	500–1600	93.50	2.695	1.066	1.08
Exit flange	360–1200	48.01	1.384	0.547	0.55
Total		918.7	26.48	10.48	10.60
Train A					
TGT A	470–1000	281.0	8.098	3.204	3.24
TGT - filter line	430	154.3	4.447	1.759	1.78
First prefilter	405	826.4	23.82	9.423	9.53
Second prefilter	405	339.9	9.796	3.876	3.92
HEPA filters	405	80.34	2.315	0.916	0.93
Total		1682	48.48	19.18	19.40
Train B					
TGT B	470–1000	1415	40.78	16.135	16.33
TGT - filter line	430	365.2	10.53	4.164	4.21
First prefilter	410	3221	92.83	36.729	37.16
Second prefilter	410	103.8	2.992	1.184	1.20
HEPA filters	410	17.5	0.504	0.200	0.20
Total		5123	147.6	58.42	59.10
Train C					
TGT C	470–1010	275.3	7.934	3.139	3.18
TGT - filter line	430	64.00	1.844	0.730	0.74
First prefilter	410	582.6	16.79	6.643	6.72
Second prefilter	410	18.67	0.538	0.213	0.22
HEPA filters	410	3.48	0.100	0.040	0.04
Total		944.0	27.21	10.76	10.89
Total in condenser and cold charcoal		0.337	0.010	0.004	0.00
Total found outside fuel		8668	249.8	98.84	100.0
Total in fuel (after test)		11.70	0.337	0.133	

[a]Inventory based on measured data: 8769.7 mCi ^{137}Cs on July 1, 1986; 0.02882 mg Cs/mCi ^{137}Cs based on ORIGEN2.

Table 8. Fractional release and distribution of ruthenium and antimony in test VI-3[a]

Location	^{106}Ru		^{125}Sb	
	μCi	Percent of inventory	μCi	Percent of inventory
Furnace components				
Inlet parts	413	0.10	91	0.10
Furnace tube	800	0.19		
ThO_2 plug	14,288	3.36	1,510	1.72
ZrO_2 plug	2,187	0.51	20,000	22.67
ZrO_2 donut	1,120	0.26	826	0.94
Exit flange	0	0.00	166	0.19
Total	18,808	4.43	22,593	25.61
Train A				
TGT A	0	0.00	0	0.00
TGT - filter line	0	0.00	0	0.00
First prefilter	0	0.00	0	0.00
Second prefilter	0	0.00	0	0.00
HEPA filters	0	0.00	0	0.00
Total	0	0.00	0	0.00
Train B				
TGT B	0	0.00	13,000	14.74
TGT - filter line	1	0.00	4,722	5.35
First prefilter	66	0.02	34,960	39.63
Second prefilter	0	0.00	0	0.00
HEPA filters	0	0.00	0	0.00
Total	67	0.02	52,682	59.72
Train C				
TGT C	20	0.00	3,858	4.37
TGT - filter line	132	0.03	967	1.10
First prefilter	2,150	0.51	6,984	7.92
Second prefilter	130	0.03	301	0.34
HEPA filters	0	0.00	56	0.06
Total	2,432	0.57	12,166	13.79
Total outside fuel	21,307	5.01	87,411	99.11
Total in fuel (after test)	380,000	89.41	781	0.89

[a]Inventories based on measured data: 425.0 mCi ^{106}Ru and 88.22 mCi ^{125}Sb.

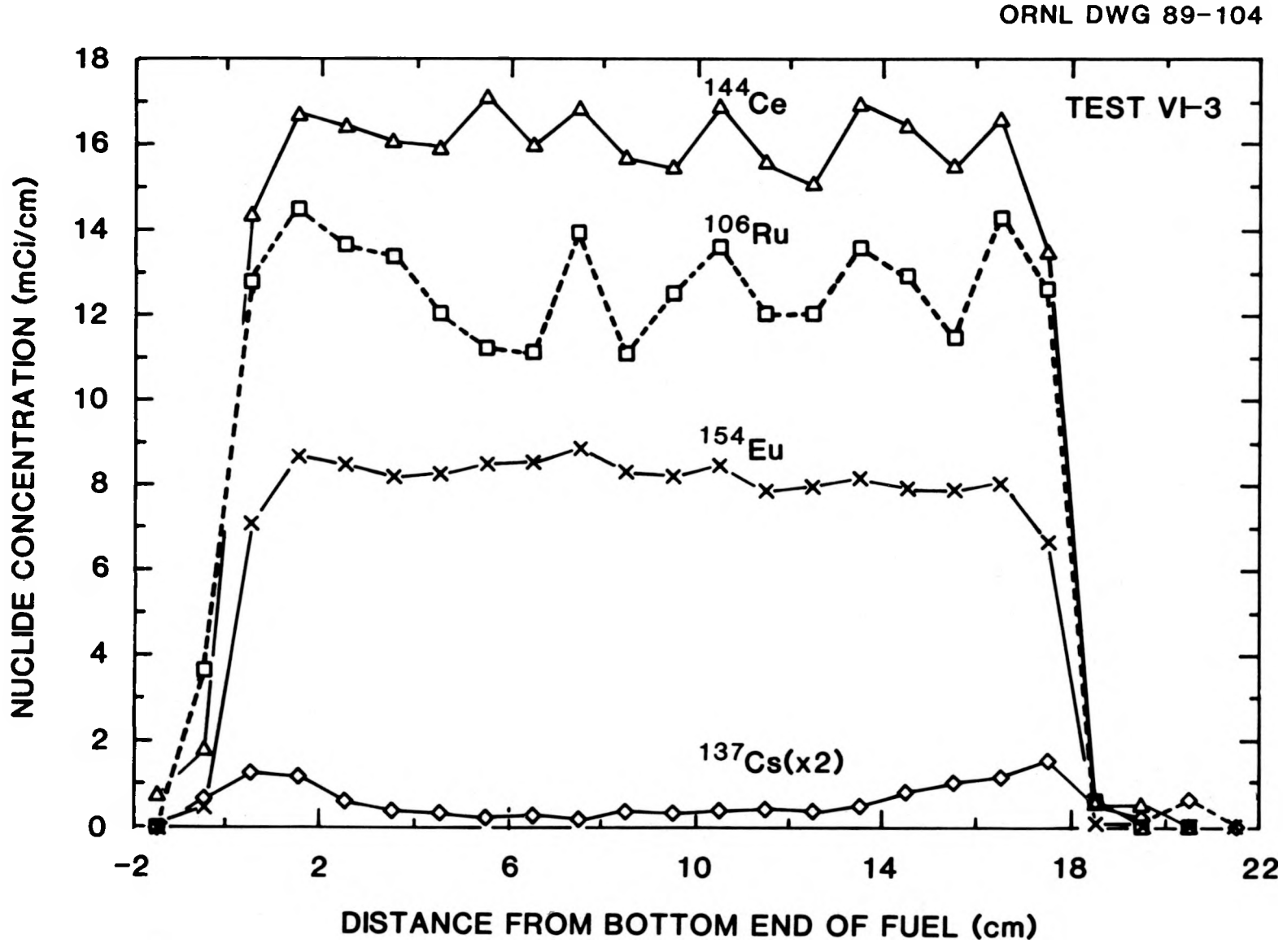

Fig. 12. Posttest distribution of major fission products in test VI-3 fuel specimen.

distribution of europium, which is relatively involatile under oxidizing conditions and has a high-energy gamma ray useful for accurate analysis, should be the best indicator of UO_2 position. (On an absolute chemical basis, cerium should be the best UO_2 indicator, but the counting statistics are much better for ^{154}Eu than for ^{144}Ce, thus making the europium more reliable.) It is significant that almost no change in the ^{154}Eu distribution occurred during the test. The two curves shown in Fig. 13, pretest and posttest distributions of europium, verify that no significant change in UO_2 fuel distribution occurred. In addition, the pretest and posttest cesium curves in Fig. 13 show that essentially all (~99%) of the cesium was released from the fuel during the test.

4.3.2 Analysis for Iodine

Since iodine has no long-lived, gamma-emitting nuclides, analytical methods other than gamma spectrometry must be used. Neutron activation of ^{129}I to ^{130}I, which can be counted easily, is a proven, sensitive technique. Iodine forms dissolve readily in basic solutions to form stable iodides, and the collector components from this test were leached to remove this iodine for analysis. Iodine adsorbed on the heated charcoal in the filter packages is analyzed by activation also. Unfortunately, no activation analyses to determine the amount of iodine in these leach solutions and on the charcoal have been possible because all reactors at ORNL have been inoperative since the test was conducted. These analyses will be carried out as soon as possible, and the results will be reported later.

An alternative method of analysis, direct counting of the ^{129}I X rays, was attempted unsuccessfully. Very small (trace) amounts of radiocesium were sufficient to prevent accurate measurement of the much weaker X rays.

4.3.3 Thermal Gradient Tube Deposits

After removal from the TGTs, the liners (liner A was pre-oxidized stainless steel and liners B and C were platinum) were analyzed by gamma spectrometry. Each tube liner was counted through 1.27- and 3.81-cm-thick lead plates to determine the total activity and then scanned with a 0.2-cm-wide collimator (continuously) and also a 1.0-cm-wide collimator (1 cm at a time) to determine the distribution of radioactivity. The abundant ^{134}Cs and ^{137}Cs were easily measured in all cases. The data from the 1-cm scans (which had no lead shielding) provided the best sensitivity for determining the amounts of ^{125}Sb. Because the lead shielding resulted in some distortion of the spectra and preferentially shielded the lower energy gamma rays, antimony (which has only relatively low energy gamma rays compared to cesium) could not be measured accurately in the through-lead counts.

The quantities and fractions of cesium and antimony found on the TGTs are shown in Tables 7 and 8. Much larger fractions (2 to 5 times more) of the cesium were found on the filters than on the TGTs,

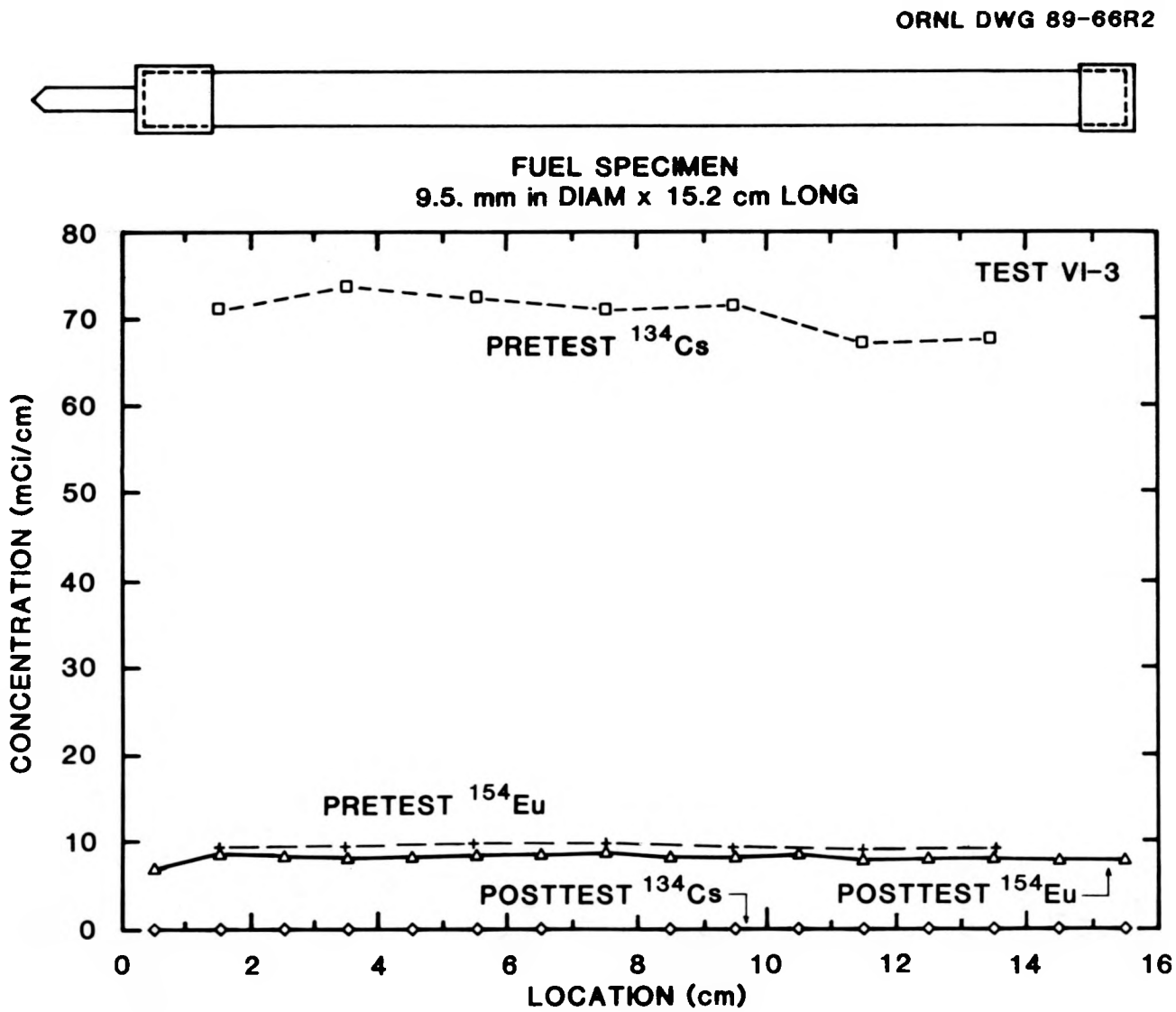

Fig. 13. Comparison of pretest and posttest distributions of cesium and europium in the test VI-3 fuel specimen.

indicating that ~75% of the released cesium was in aerosol rather than vapor form. This observation is in agreement with previous tests in steam.[11,12]

The profiles of cesium and antimony for the three TGT liners, and also the temperature profiles, are shown in Figs. 14 and 15. Thermal gradient tube A was stainless steel which had been oxidized (by heating to 750°C in steam) at the beginning of the test to provide a surface more typical of those in a reactor coolant system. Note that no antimony was found in TGT A. A delay in the release of antimony until most of the Zircaloy cladding had been oxidized would be expected because previous tests have shown that antimony is retained in metallic Zircaloy.[11,12] As shown in Fig. 14, the concentrations of cesium were much higher in TGT B than in the other two TGTs; this result is consistent with the total release data in Table 7, which shows the distribution of total cesium release in Phases A, B, and C to be 19%, 59%, and 11%, respectively. It appears that the very high cesium peak at the entrance of TGT B is at too high a temperature (~700°C) to be primarily either CsI or CsOH. (In previous tests, cesium peaks at deposition temperatures of ~500°C have been observed and have been attributed to these compounds.) In this test, another form of cesium (perhaps $CsMoO_4$, since a large amount of molybdenum was found on the Train B filters) is believed to be responsible for the peak at higher temperature. As observed in previous tests, most of the CsI and CsOH were believed to be deposited in the broad cesium peaks at lower temperatures, especially in TGT B where the largest fraction of cesium was found. The distribution of cesium in the oxidized stainless steel TGT A (Fig. 14) was not markedly different from cesium distribution in platinum TGT liners.

4.3.4 Results of Spark Source Mass Spectrometry (SSMS) Analyses

Small smear samples of the material deposited on the filters were collected on graphite electrodes and analyzed by SSMS. This technique has advantages in that it is very sensitive not only for the radionuclides but also for the stable elements, including structural materials and any impurities in the system. Its disadvantage is its relatively low precision, a factor of 2 to 3. These data may be converted to absolute values by comparison with either the ^{137}Cs data or known standards of erbium injected during the vaporization step.

The results of SSMS analyses of samples from the test VI-3 filters are summarized in Table 9. These data were normalized to the masses of material determined by weighing (Sect. 4.3.7); milligrams of element and percentage of total are shown for each sample. For test Phase A (20 min at 2000 K), the fission products Cs and Rb (56% of the total) dominated the release, followed by the cladding elements Zr and Sn (19%). For the higher temperatures during Phases B and C, however, most of the cladding had been oxidized, and uranium comprised 64% and 92% of the released mass, with significant contributions from Cs, Mo, Te, and Sn. The

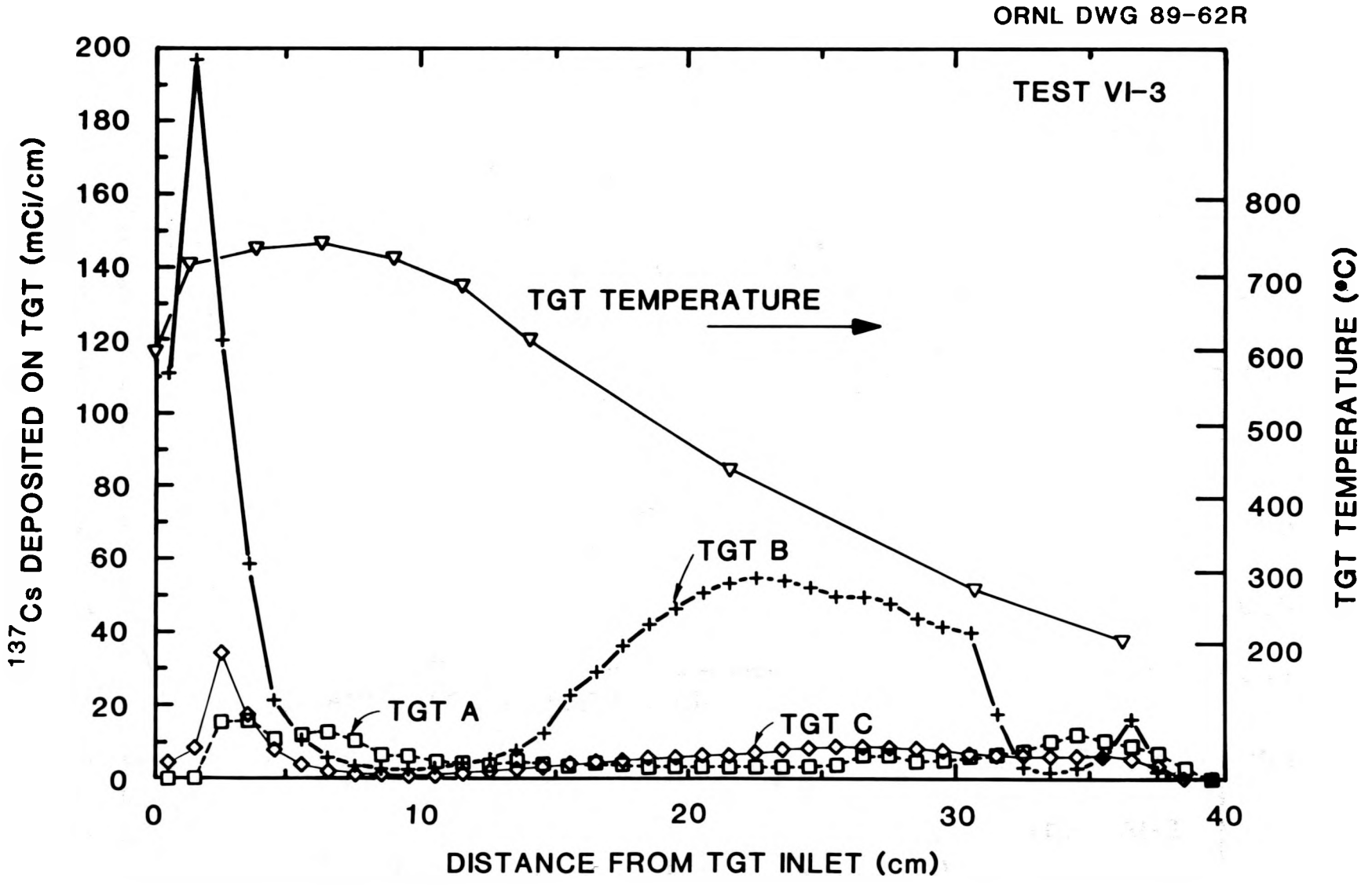

Fig. 14. Distributions of cesium in thermal gradient tubes A, B, and C.

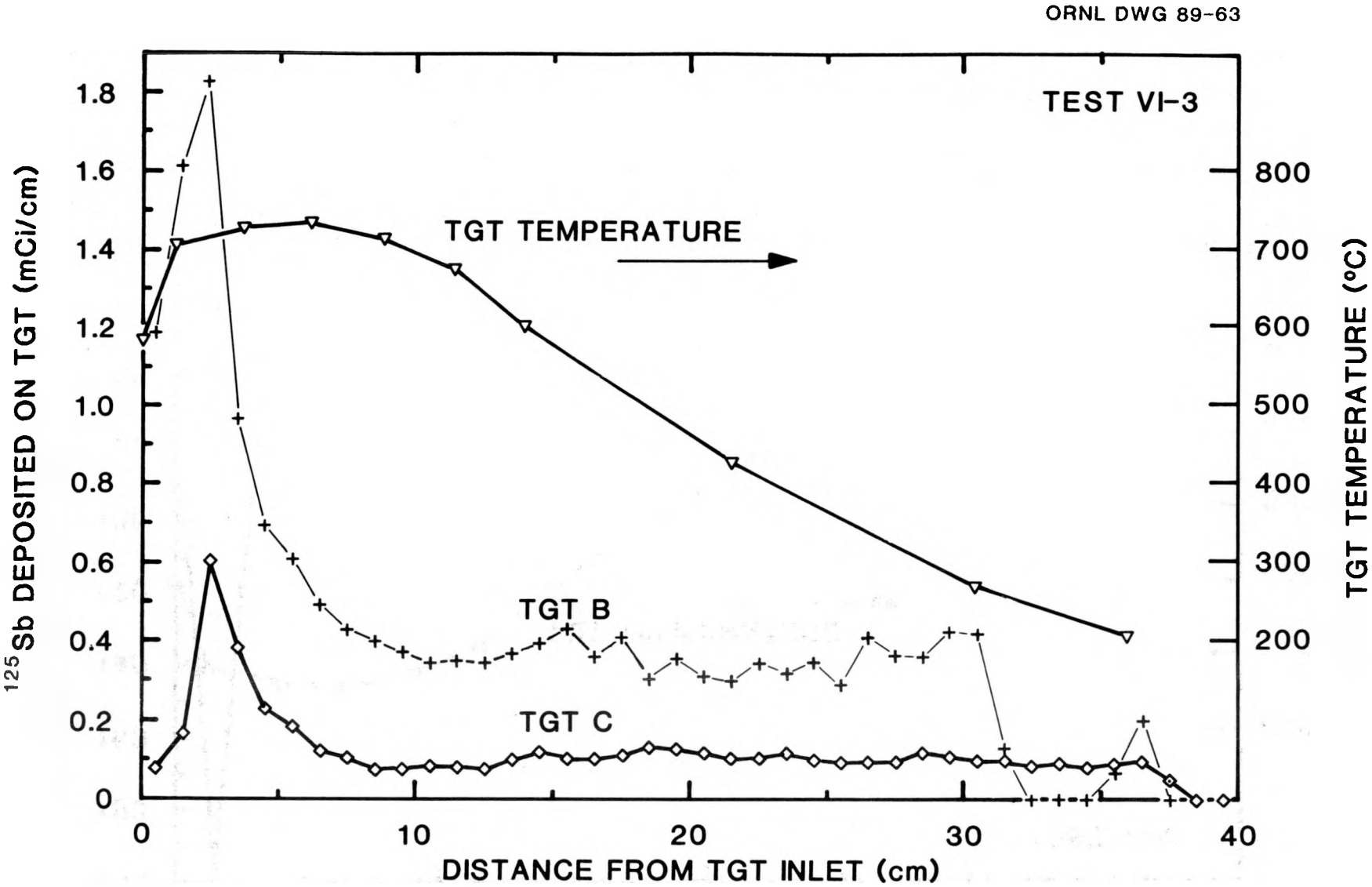

Fig. 15. Distributions of antimony in thermal gradient tubes B and C.

Table 9. Spark source mass spectrometry data for test VI-3[a] (data normalized to total mass on filters, and assuming 20% of the mass was oxygen)

Fission products[b]	Train A prefilter		Train B prefilter		Train C prefilter	
	(mg)	(%)[c]	(mg)	(%)[c]	(mg)	(%)[c]
Cs	60.0	50.0	20.0	4.0	5.0	0.8
Mo	2.0	2.0	70.0	10.0	20.0	3.0
Pd	0.0	0.0	30.0	5.0	4.0	0.7
Rb	9.0	7.0	5.0	0.7	0.8	0.1
Te	0.0	0.0	10.0	2.0	0.0	0.0
Tc	0.0	0.0	7.0	1.0	5.0	0.8
I	0.0	0.0	0.0	0.0	0.0	0.0
Total	70.0	60.0	100.0	20.0	30.0	6.0
Reactor materials[b]						
U	0.0	0.0	400.0	60.0	600.0	100.0
Sn	3.0	2.0	90.0	10.0	8.0	1.0
Zr	20.0	20.0	0.0	0.0	0.7	0.1
Fe	8.0	7.0	4.0	0.6	3.0	0.5
Ni	1.0	0.9	0.0	0.0	0.6	0.1
Cr	0.0	0.0	0.5	0.1	0.9	0.2
Mn	0.1	0.1	0.0	0.0	0.0	0.0
Ag	0.0	0.0	1.0	0.2	0.5	0.1
B	0.0	0.0	0.0	0.0	0.2	0.0
Total	30.0	30.0	500.0	100.0	600.0	100.0
Other materials[b]						
Th	8.0	7.0	0.0	0.0	0.0	0.0
Ca	2	1	3	0.5	0.6	0.1
Y	3.0	3.0	0.0	0.0	0.0	0.0
Al	0.7	0.6	0.5	0.1	0.4	0.1
Cl	0.0	0.0	1.0	0.2	0.3	0.0
Cu	2.0	2.0	0.0	0.0	0.0	0.0
Pb	1.0	0.9	0.0	0.0	0.0	0.0
K	0.9	0.8	0.0	0.0	0.3	0.0
Na	0.0	0.0	0.2	0.0	0.3	0.0
P	0.0	0.0	0.0	0.0	0.1	0.0
Total	20.0	10.0	5.0	0.8	2.0	0.3
Total all	100.0	100.0	700.0	100.0	600.0	100.0

[a]Precision of all data is about a factor of 2; shown to one significant figure only.

[b]In approximate order of abundance.

[c]Percentage (by mass) of element in sample.

discrepancy in relative cesium release between Phase A and Phase B (compared to the gamma data in Sect. 4.3.1) is believed to be a result of non-representative samples, but also indicates the limitations in using data from this low-precision method.

4.3.5 Results of Inductively Coupled Plasma-Emission Spectrometry (ICP-ES) Analyses

Samples of the acidic leach solutions from the filters were submitted for ICP-ES analysis for non-gamma-emitting elements. This technique is best suited for measuring cations. Although it is unfortunately not useful for I analysis, it appeared promising for the measurement of Mo, Te, Ba, and perhaps for U. Because of the high levels of radiocesium in all samples, large dilutions were required to avoid excess radiation dose to the analyst. Unfortunately, these large dilutions resulted in poor sensitivities for measuring the elements of interest. The sensitivity for Te was found to be disappointingly low, but useful data for Mo, Ba, and U were obtained.

The results from ICP-ES analyses of test VI-3 filter samples are summarized in Table 10. The limits of sensitivity are indicated by less than (<) values. Measurable amounts of Ba and Sn (most of the Sn comes from the Zircaloy cladding) were found in all cases, and Mo and U were measured in the higher concentration samples. Fractional release values for the fission products and uranium were determined where possible. These indicated that ~14% of the barium and ~2% of the molybdenum were released to the filters. These values for barium, especially the indicated 2% release during test phase A, seem surprisingly high and must be considered preliminary until confirmed. With further work, we are optimistic that this technique will prove valuable in evaluating fission product release from these tests.

4.3.6 Uranium and Plutonium Data

Since the release and transport of fuel material (uranium and plutonium) provides a potential mechanism for the release of low-volatility fission products (by association with the heavy-fuel atoms) in addition to the direct hazard of the heavy metals, the determination of fuel release is important. The data, obtained by fluorimetric analysis for uranium and by alpha particle analysis for plutonium of deposits from the filters, are summarized in Table 11. These data indicate that <1% of the uranium and <0.001% of the plutonium escaped from the furnace to the filters, with almost all of this being released during the very high temperature period (Phases B and C) of the test.

Uranium release was measured by two other techniques; these data are shown in Table 12. As indicated, the ICP-ES data agreed well with the fluorimetric data, but the SSMS data were high by a factor of ~2. Since no better precision is claimed for SSMS, this lack of agreement is not surprising.

Table 10. Release data for test VI-3 obtained by inductively coupled plasma-emission spectrometry analysis

Sample location	Fuel conditions	Element	Mass found[a] (μg)	Release[b] (%)
Train A filters	Heatup + 20 min at 2000 K	Ba	3.09	2.034
		Mo	<0.018	
		Sn[c]	2.50	
		Te	<1.0	
		U	<1.7	
Train B filters	Heatup, 2000 to 2700 K, + 1.5 min at 2700 K	Ba	12.6	8.312
		Mo	6.9	2.240
		Sn[c]	45.2	
		Te	<30	
		U	166	0.248
Train C filters	18.5 min at 2700 K + cooldown	Ba	6.03	3.966
		Mo	<2.8	
		Sn[c]	5.43	
		Te	<15	
		U	332	0.497
Totals		Ba	21.8	14.311
		Mo	6.92	2.240
		U	497	0.745

[a]Limits of sensitivity shown by < values.
[b]Fuel inventories: Mo = 309.1 mg; Ba = 152.1 mg; U = 67.76 g.
[c]Tin was present primarily as a component of the Zircaloy cladding.

Table 11. Release of uranium and plutonium in test VI-3[a]

Location	Uranium		Plutonium		
	mg	Percent of inventory	μg	Percent of inventory × 10E3	ppb[b]
Train A	0.312	0.00046	0.0174	0.003	30
Train B	167	0.247	0.0492	0.0084	84
Train C	298	0.440	0.198	0.034	340
Total	465.3	0.687	0.265	0.0454	454

[a]Inventories in fuel after irradiation: 67.72 g U and 0.583 g Pu.
[b]ppb = parts per billion.

Table 12. Uranium release in test VI-3: comparison of data from different measurement techniques

Collection train	Mass U (mg)			Percentage of inventory[d]
	SSMS[a]	ICP-ES[b]	Fluor.[c]	
A	0	<1.7	0.312	0.00046
B	434	166	167	0.247
C	562	332	298	0.440
Total	996	498	465	0.687

[a]SSMS = spark source mass spectrometry, average of two solid samples.

[b]ICP-ES = inductively coupled plasma-emission spectrometric analysis of acidic leach solution.

[c]Fluor = fluorimetric analysis of acidic leach solution.

[d]Based on fluorimetric data, which is the most accurate of the three methods.

4.3.7 Masses of Deposits in TGT and on Filters

Each filter and TGT liner was weighed before and after the test to determine the mass of material collected during the test. Immediately after disassembly of the filter packages, the filters were inspected and photographed, then packaged for weighing. Both prefilters and the first high-efficiency particulate absolute (HEPA) filter exhibited deposits, but no deposits were visible on the last HEPA filter, indicating efficient collection of most of the aerosols by the previous filters. The masses of material collected at the various locations are listed in Table 13 and illustrated in Fig. 16. As would be expected, the greatest masses were collected during Phases B and C, at the highest temperatures, and the total mass collected (3.17 g) was greater than in any previous test.

Most of the material deposited in the TGT liners is believed to be a result of vapor condensation, and the material deposited on the filters probably was transported primarily as aerosol. The average mass concentration of vapor and aerosol during each test phase was calculated from the masses collected and the total gas flow during that period (see Table 13). To reduce the distortion of the heatup and cooldown periods, it was assumed that no aerosol was formed at temperatures below 1900 K. These data show that the average mass concentration of the aerosol was highest during test Phase B and that this average mass concentration declined during the test as the supply of the more volatile material was depleted.

4.3.8 Fuel Examination

As noted previously, the fuel specimen was cast in epoxy resin to preserve the test geometry before removal from the furnace. The surrounding ThO_2 furnace tube was broken away from the epoxy, allowing limited viewing of the fuel through the translucent epoxy. The specimen was packaged and shipped to SNL for X-ray inspection; this image, shown in Fig. 10, revealed good agreement of physical features such as pellet gaps with the posttest gamma scan. Subsequently, the specimen was shipped to ANL, where it was cut with an abrasive saw for examination of the fuel cross sections. Two representative sections (at ~1 cm and ~10.5 cm from the bottom end of the specimen) were selected and prepared for metallographic examination. These sections are shown in composite form in Figs. 17 and 18. In the lower section (Fig. 17), it is immediately apparent that the Zircaloy cladding was completely oxidized, and that a large cladding fracture had occurred. However, the wall thickness of the oxidized Zircaloy is too thick (by a factor of nearly 2) relative to the rod diameter, suggesting that this section included the bottom end cap, which had a wall thickness similar to that of the cladding. The large gap between the fuel and the cladding and the irregular, porous outside surface of the fuel pellet also represent significant changes from the untested state. The rounded surfaces of the fracture could have resulted from reaction (oxidation and vaporization) with the flowing steam.

Table 13. Vapor and aerosol deposits in test VI-3

	Weight of deposits (g)[a]			
	Train A	Train B	Train C	Total
Thermal gradient tube (TGT)	0.061	0.380	0.241	0.682
Filters:				
Prefilter 1[b]	0.168	0.967	0.978	
Prefilter 2	0.079	0.066	0.064	
HEPAs	0.061	0.061	0.042	
Total filters	0.308	1.094	1.084	2.486
Total TGT and filters	0.369	1.474	1.325	3.168
Aerosol concentration[c] (g/m^3)	5.2	15	12	11

[a]Precision = ±0.003 g.

[b]Includes estimated mass of deposits in connecting tubes, based on ^{137}Cs data.

[c]Assumes all aerosol was formed at temperatures ≥1900 K and that the average temperature in the TGTs and filters was 423 K.

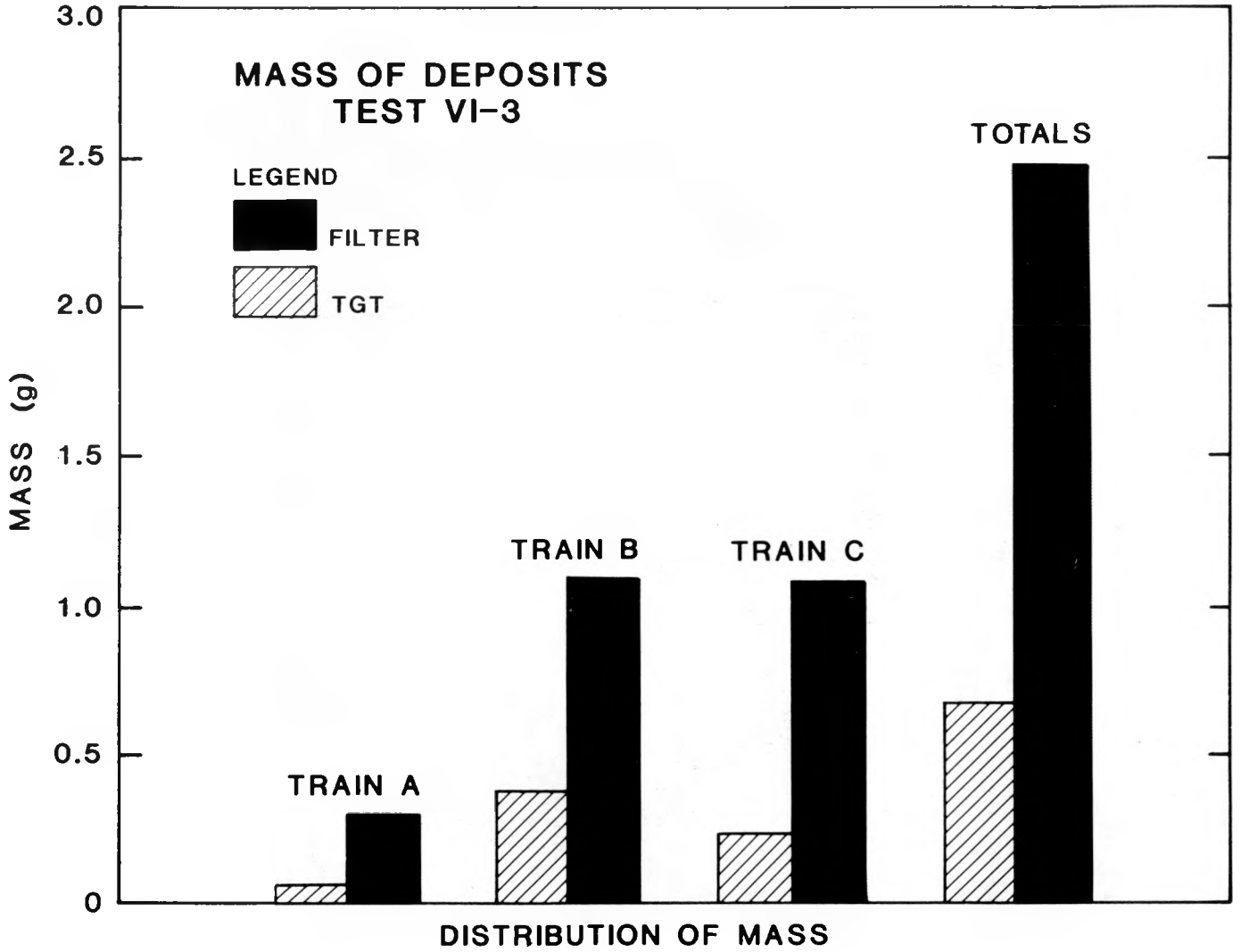

Fig. 16. Distribution of deposits collected on TGTs and filters in test VI-3.

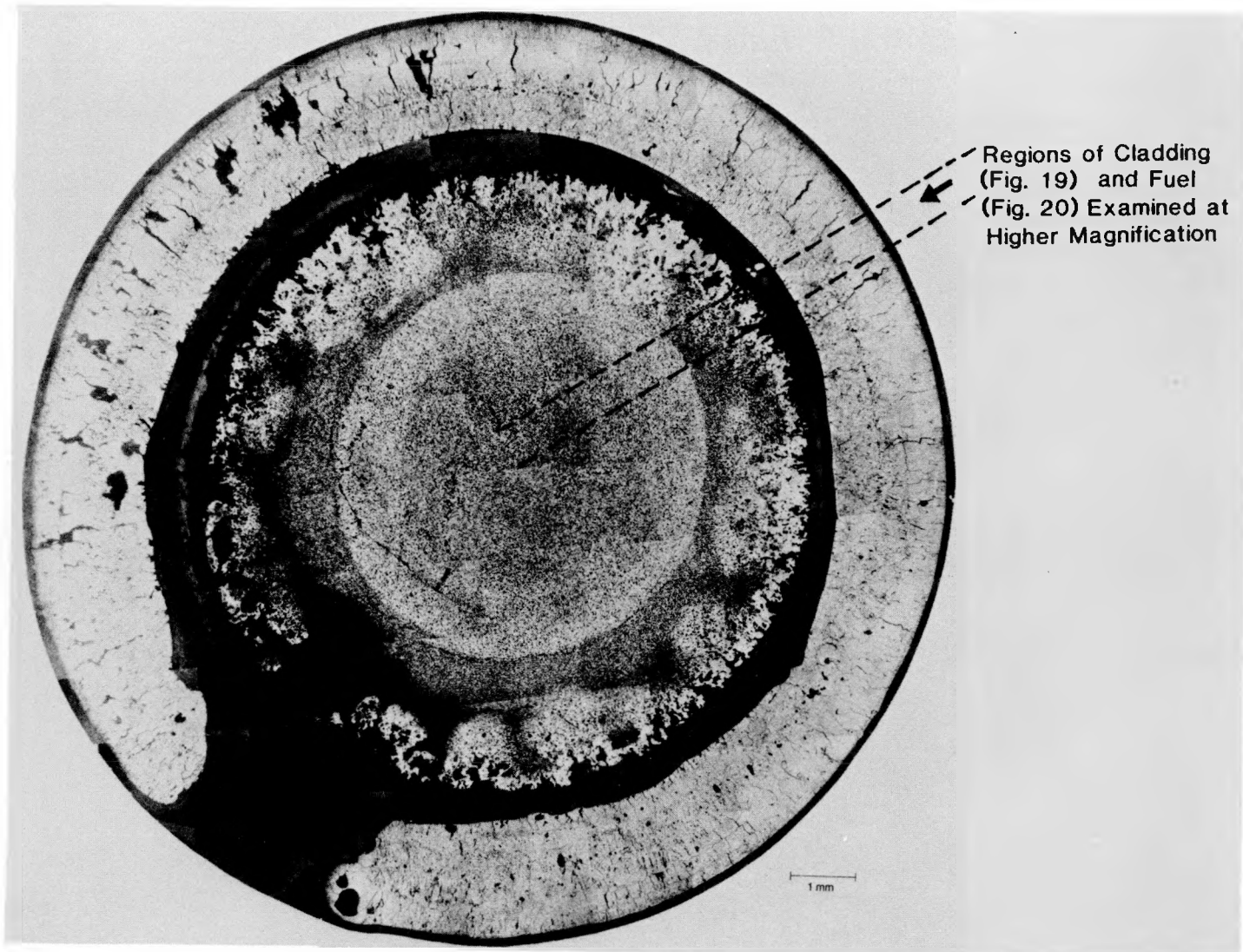

Fig. 17. Cross section of fuel specimen from test VI-3 at ~1 cm from the bottom end.

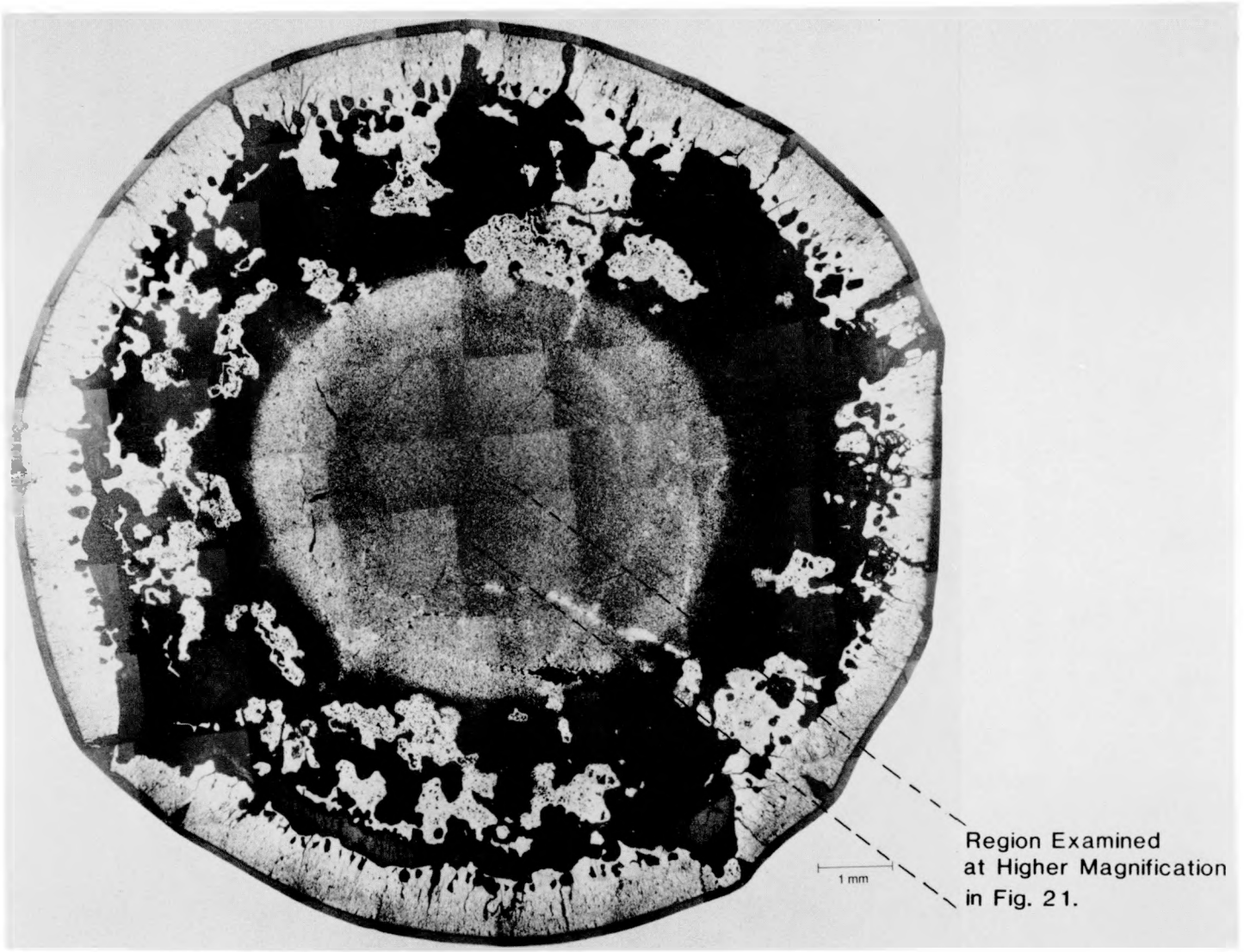

Fig. 18. Cross section of fuel specimen from test VI-3 at 10.5 cm from the bottom end.

A higher magnification view of an oxidized Zircaloy section (apparently both cladding and end cap) is shown in Fig. 19. Although a section just above the bottom end cap was intended, the relative thickness of the oxidized Zircaloy and the ring of pores at about mid-thickness (as shown in Fig. 17) indicate that the radial cut was slightly below the intended location and actually included the end cap. The extensive microfracturing and/or grain separation within this specimen is typical of Zircaloy oxidized under the conditions of this test (i.e., at high temperature in steam). The appearance of the UO_2 fuel may be seen better in the higher magnification views across the fuel radius in Fig. 20. A change in the porosity and/or gas bubble morphology from the OD to the center of the fuel is apparent. The largest bubbles are seen only near the surface of the UO_2. In the region of the center, the pores are closer together and frequently are interconnected. Coalescence of the gas bubbles during the high-temperature test and random migration toward the irregular surface of the UO_2 where they could be released appears to explain these observations.

In addition, numerous small metallic inclusions were observed in Fig. 20. Based on previous work, we suspect that these inclusions are mixtures of metallic fission products, such as molybdenum, technetium, ruthenium, and palladium.[21] Under the high-temperature, highly oxidizing conditions of this test, however, some of these fission products (molybdenum, for instance) may have been evolved from the fuel. The cause of the large fuel-cladding gap is believed to be steam reaction with the UO_2 and vapor transport to other (cooler) regions within the fuel specimen and test apparatus. (Post-fracture opening of the cladding is a possible alternative or partial explanation, but is believed to be less likely. Such a large opening or spreading of the cladding, which apparently occurred during the oxidation process, was seen in test HI-2.)[22] Liu reported that calculations at ANL by SOLGASMIX indicated that as much as a few percent of the UO_2 could have been vaporized under the conditions of this test.* As noted in Sect. 4.3.6, significant amounts of uranium were measured on the filters, and similar or larger amounts could have been transferred to other, unsampled locations within the test apparatus. The very irregular features of the UO_2 surface are apparent in both Figs. 17 and 20. The ingress of steam at the cladding fracture in Fig. 17 appears to have resulted in accentuated reaction/vaporization of the adjacent UO_2, with progressively less loss of UO_2 as the distance increases from the entry point of the steam. Furthermore, the fuel-cladding gap is even larger in Fig. 18. The slightly higher temperature in this region (~50 K as indicated by pretest temperature calibrations and by the posttest cesium profile in Fig. 12) would have contributed to a higher vaporization rate.

---

*Y. Y. Liu, Argonne National Laboratory, private communication, November 1989.

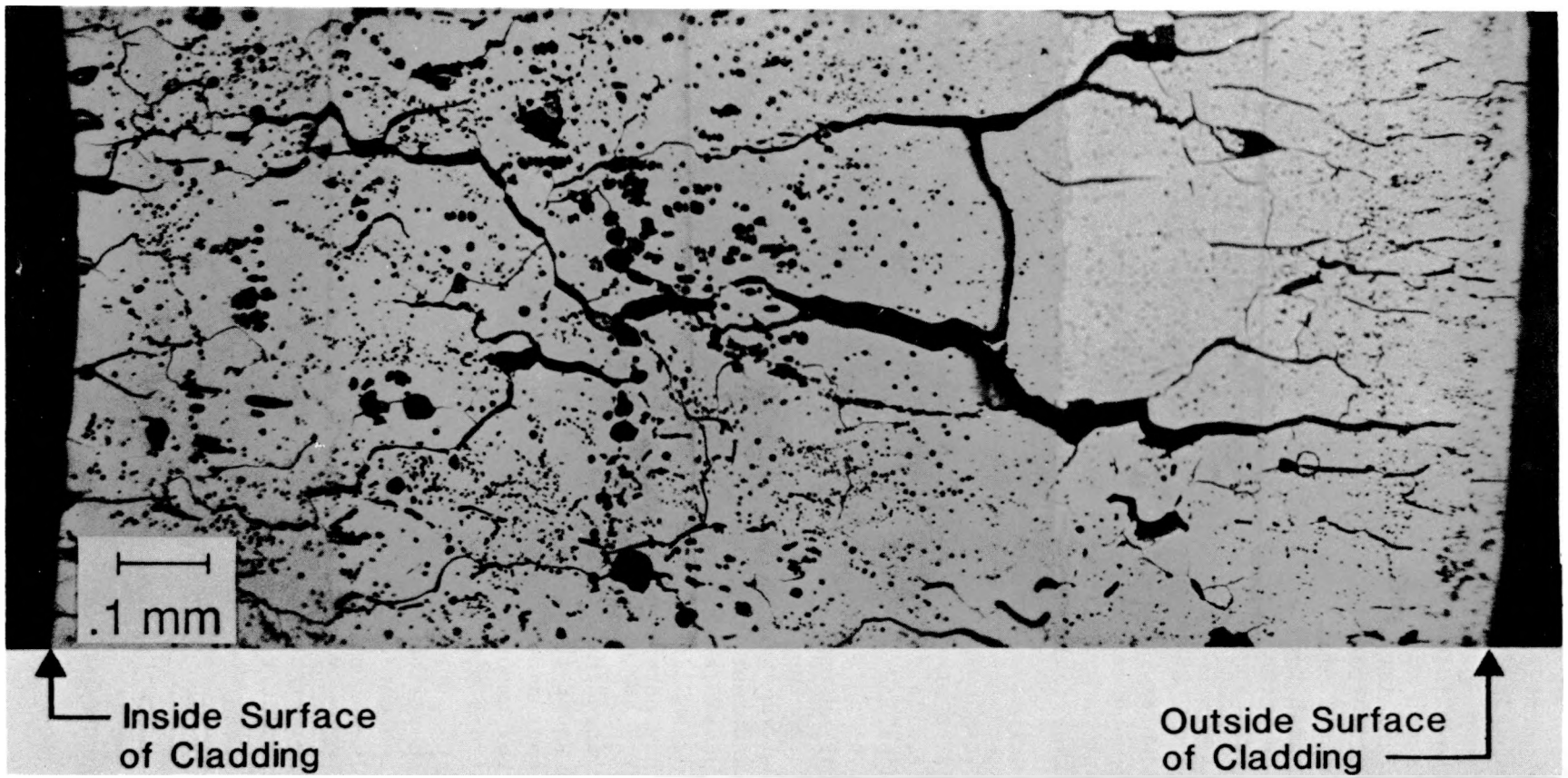

Fig. 19. Higher magnification view of oxidized cladding from Fig. 17.

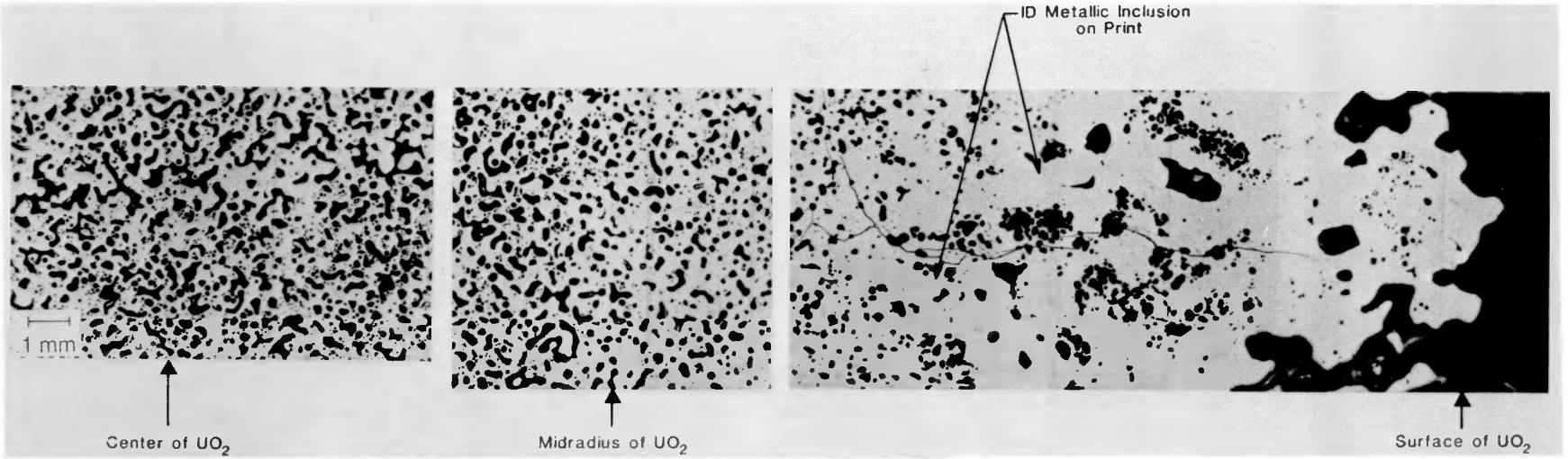

Fig. 20. Higher magnification view of fuel from Fig. 17, adjacent to cladding in Fig. 19.

Differences in the appearance of the fuel and cladding at 10.5 cm above the bottom end (Fig. 18), compared to that in Fig. 17, are readily apparent, but are not well understood. Again, the cladding was completely oxidized with multiple fractures, and, in addition, the interior surface of the cladding was very irregular, perhaps evidence of significant fuel-cladding interaction. The pieces of material between the oxidized cladding and the remaining UO_2 were composed of oxide mixtures of zirconium and uranium, and lighter-colored stringers of zirconium-rich material had penetrated significant distances into the UO_2 along fracture lines. These features, along with the apparently smaller diameters of several fuel pellets as seen in the X-ray image (Fig. 10), indicate that some fuel-cladding interaction, in addition to fuel evaporation, had occurred. Without fuel-cladding interaction in this region, it would be difficult to explain the obvious differences in morphology of the UO_2. In Fig. 17 the UO_2 near the surface is high in density with many deep penetrations, whereas in Fig. 18 it is more uniform but of lower density. If the intruding steam was the primary vehicle for vaporization and transfer of the UO_2 in both areas, more similar morphologies would be expected. The main body of UO_2 is much larger in diameter in Fig. 17, apparently near the original pellet diameter. This indicates that less fuel erosion, whether by steam oxidation/vaporization or by fuel-cladding interaction, occurred near the bottom end of the fuel specimen than near midlength (Fig. 18).

Examination of the higher magnification views of the upper section in Fig. 21 provided more detailed views of the fuel-cladding interaction region. Electron microprobe analyses showed that fuel material was in contact with the oxidized cladding, and that the concentration of uranium in the (U,Zr)O mixture increased (and the concentration of zirconium decreased) with distance away from the cladding. Very few of the white inclusions believed to be high concentrations of metallic fission products, which were numerous in Fig. 20, could be seen in Fig. 21. The central region of the UO_2 (shown in Figs. 18 and 21) was uniformly very porous, suggesting the coalescence of fission products that would be gaseous at the high temperature of this test (2700 K).

5. COMPARISON OF RELEASE DATA WITH PREVIOUS RESULTS

The fission product release data from this test (VI-3) have been compared with the results from earlier experiments, and also with results from a comprehensive NRC review of all relevant (but older) fission product release data.[23] The fractional releases of antimony and cesium for each phase of tests VI-1, VI-2, and VI-3 are shown graphically in Fig. 22. Test conditions are listed in Table 14. The trend to higher release with higher temperatures and increasing time in these tests is apparent. Although the fuel in test VI-2 was maintained at 2300 K for a longer time than that in test VI-1 (60 min vs 20 min), the total cesium release was the same, 63%. The different types of fuel and different irradiation conditions - Oconee in VI-1 and BR3 in VI-2 - are the only apparent reasons that more cesium was not released in test VI-2. In test VI-3 at 2700 K, the largest releases of both antimony and

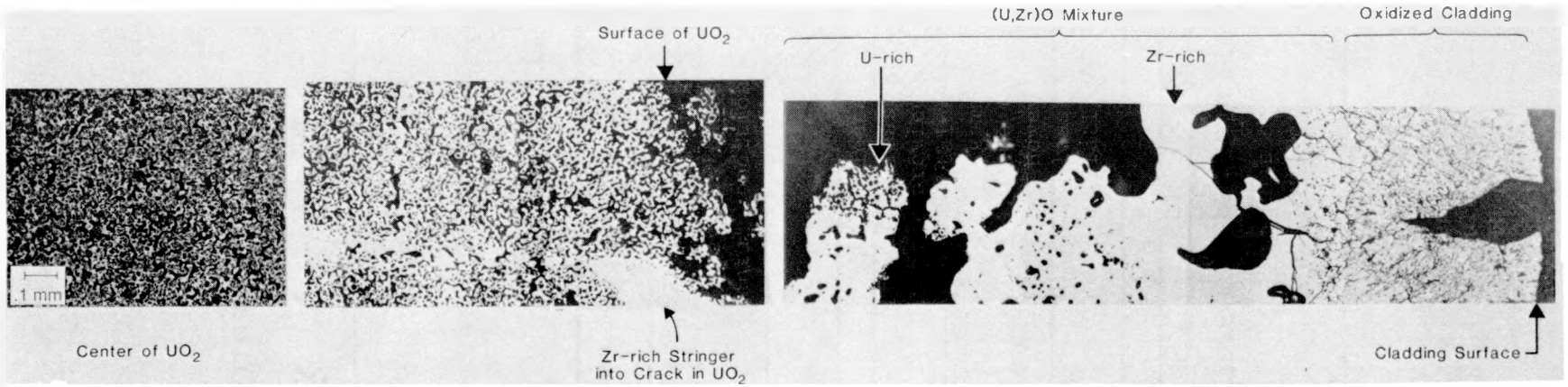

Fig. 21. Higher magnification view of fuel from Fig. 18.

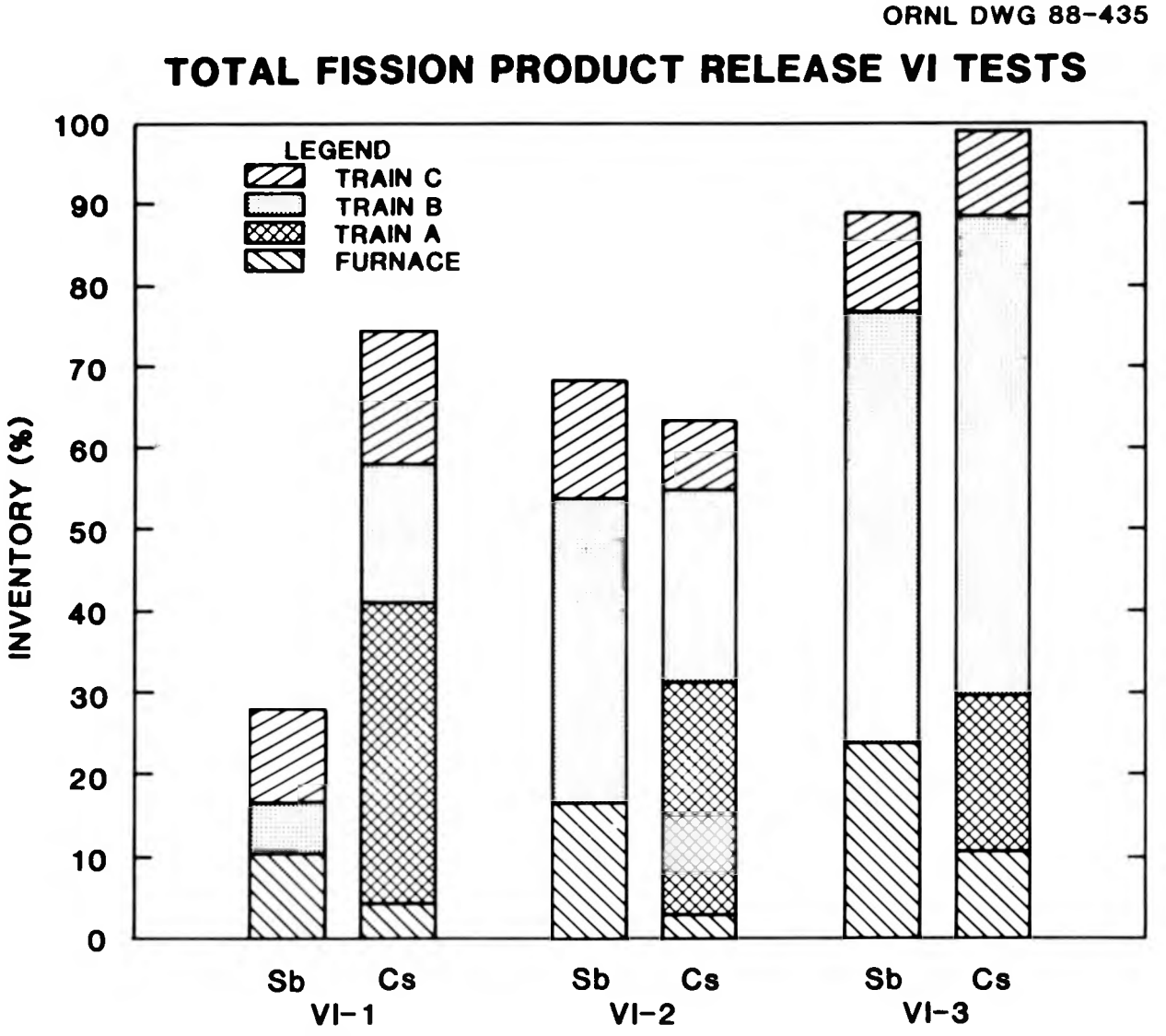

Fig. 22. Comparison of strontium and cesium release in tests VI-1, VI-2, and VI-3.

Table 14. Comparison of krypton and cesium release data from HI and VI tests

Test no.	Test conditions				Percent released	
	Fuel	Temperature (K)	Effective time[a] (min)	Steam flow rate[b]	Kr	Cs
HI-2	HBR	2000	22.5	High	51.8	50.5
HI-5	Oconee	2000	21.5	Low	19.9	20.3
VI-1A	Oconee	2020	25.5	High	c	28.7[d]
VI-3A	BR3	2000	34	High	26.0	21.7[d]
VI-1B	BR3	2300	14	High	c	17.5[d]
VI-1C	BR3	2300	19	High	c	16.9[d]
VI-2A	BR3	2300	5	High	c	29.7[d]
VI-2B	BR3	2300	18	High	c	24.5[d]

[a]Includes estimates for heatup and cooldown effects.

[b]Test atmosphere was either strongly oxidizing throughout test (high) or transient conditions: oxidizing and reducing (low).

[c]No intermediate values for krypton release during the test were obtained, should be similar to cesium values.

[d]Assumes same distribution on furnace ceramics during test phases A, B, and C as on collection trains after test, and no contribution for release during cooldown.

cesium occurred during the 32-min transition period from 2000 to 2700 K, leaving relatively small fractions available for release at the maximum temperature. It is apparent in all three experiments that, although large fractions of cesium were released during phase A (collected on train A), very little antimony was collected on train A (Table 6 and Fig. 22). This may be explained by the expected retention of the released antimony by the metallic Zircaloy cladding until it became fully oxidized, thereby allowing the antimony to be released rapidly during phase B.

We were particularly interested in comparing the results from test VI-3 with data from similar tests in a horizontal furnace. Two of the tests in the horizontal furnace (HI-2 and HI-5) were conducted with a temperature/time regime similar to phase A in test VI-3. In addition, Phase A of test VI-1 experienced similar conditions. The release data from test VI-3 are compared with these three earlier tests in Table 14. As these data indicate, the fractional releases of krypton and cesium varied considerably. First, as was seen in all six tests in the HI series, there was very good agreement between krypton and cesium release in tests HI-2 and HI-5.[22] In test VI-3A, somewhat greater release of krypton than of cesium was indicated, but this could be explained by a delay in cesium movement from the furnace to the collectors where it could be monitored. In test VI-1A, however, no krypton data are available for comparison with the cesium data. (No measurement of krypton collection at the end of test phase A was obtained.)

Considering the differences in fuel history (H. B. Robinson in test HI-2, Oconee in HI-5 and VI-1, and BR3 in VI-3) and in steam availability (low in HI-5 and high in HI-2, VI-1, and VI-3), the agreement in cesium release values from tests HI-5, VI-1A, and VI-3A is reasonably good. The cesium release in test HI-2, however, was much higher - 50% vs an average of 24% in the other three tests. Similarly high releases of krypton and iodine were observed in test HI-2, and these high releases have been attributed to significant oxidation of the UO_2 fuel during the test.[21] In test phase VI-1A, the fuel had been heated already at 2020 K for 20 min, thereby releasing a large fraction (39%) of the total cesium, which we conclude was located in more readily releasable sites. Consequently, much less cesium remained in the fuel, and the release rate for this remaining cesium was much lower in test VI-1 (B+C) than in test VI-2 (A+B). The higher value for total cesium release in test VI-1 (74.3%) compared to test VI-2 (63.4%) may have been related to differences in fuel morphology resulting from different irradiation histories of the fuel specimens. These data show that in both tests, the cesium tended to be released early in the high-temperature period.

The minute-by-minute total release values for cesium, which are shown in Fig. 11, were used to calculate the corresponding release rate coefficients,

$$k = -(1/t)\ \ln(1-F)\ ,$$

where t = time at temperature and F = the fractional release of the inventory during that time period. The logs of these coefficients (individual points) are plotted as a function of temperature in Fig. 23 and are compared with the release rate coefficients (curve) based on the ANS 5.4 Standard for fuel irradiated to a burnup of 42 MWd/kg.[24] The vertical clusters of points in this figure reflect the the 20-min periods at constant temperature, 2000 and 2700 K. The values of the points in these clusters declined with time at that temperature, showing a decrease in the release rate with fraction released, as was observed in test VI-2.[12]

The release rates of cesium in the three vertical tests (VI-1, VI-2, and VI-3) are compared with similar data from the six HI tests, and with the NRC review curve in Fig. 24. Because the VI tests were conducted in three phases, compared to only one phase in the HI tests, each VI test provided three release rate values. In test VI-1, these three data points were plotted for three different effective temperatures (see Fig. 24). The "effective temperature" is the true temperature adjusted slightly to account for the time at a somewhat lower temperature that would nevertheless influence fission product release. Like most of the HI test data, the cesium release rate from the vertical tests falls significantly (by factors of 3 to 20) below the CORSOR-M curve.[25] For test VI-2, which experienced only one extended test temperature, the early release rate values were comparable to the HI test data, and then showed a steady decline, by more than a factor of ten, during the test. The data points for VI-3B and VI-3C are at higher temperature than the previous data, but continue the trend of being significantly below the CORSOR-M curve. It is apparent that the B and C points for test VI-3 in Fig. 24 lie further below the CORSOR-M curve than the A point does. This illustrates the same relatively lower values for the release rate coefficients at higher temperature (or at higher fractional release from the fuel) that were shown in Fig. 12.

6. CONCLUSIONS

In view of the preliminary nature of this report and the fact that some important analyses and results have not yet been obtained, a thorough interpretation of the results of test VI-3 is impossible at this time. Upon completion of the currently delayed work, such interpretation will be published. However, several significant observations are now appropriate.

1. All of the test equipment operated well, and the planned test conditions were accomplished. This was the highest temperature test to date: 2700 K for 20 min in steam in phase C. The apparatus for the continuous measurement of hydrogen operated very well, proving its usefulness as an aid in the interpretation of test results. The test was considered successful, and the test apparatus and technique are suitable for future tests of this type.

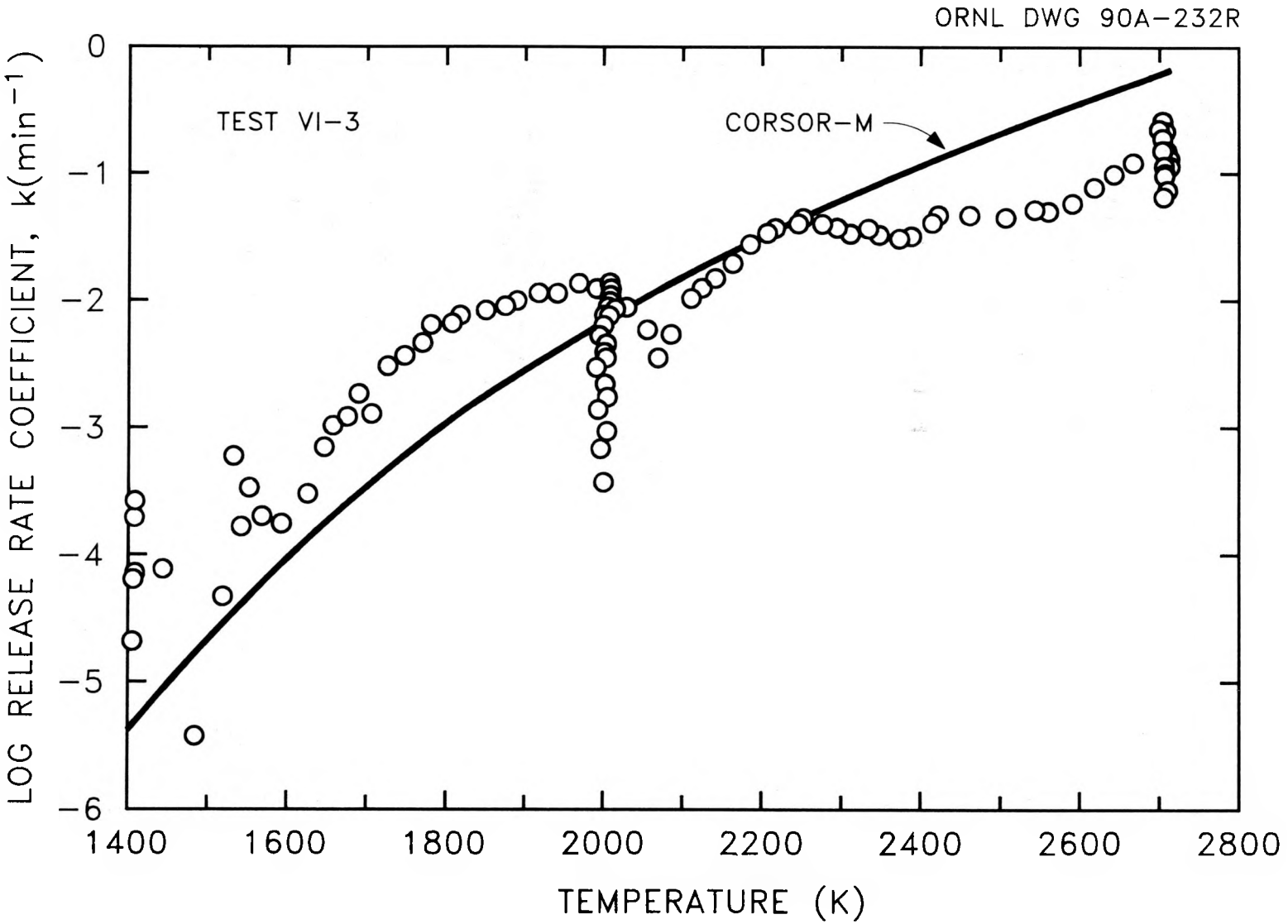

Fig. 23. Measured release rate coefficients for cesium in test VI-3, compared with ANS-5.4 standard for similar conditions.

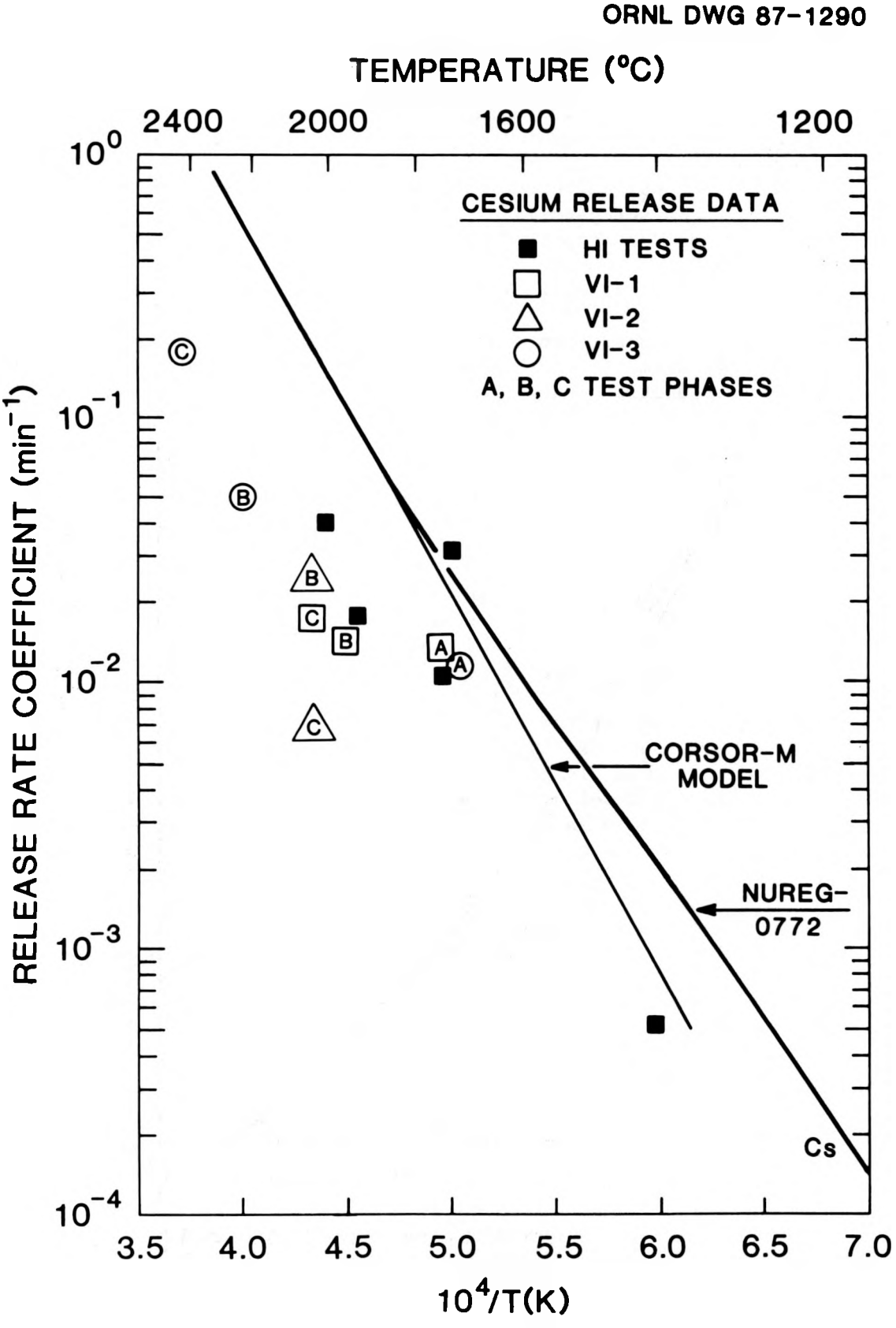

Fig. 24. Comparison of release rate coefficients from all HI and VI tests with CORSOR-M.

2. The total release values for the more volatile fission products - Kr, Sb, and Cs - were determined for the specific conditions of this test. The release values were 100% for Kr, 99% for Cs, and 89% for Sb. Comparison of the data from the first phase of test VI-3 with the results from similar previous tests showed some differences, but different experimental conditions appear to explain the discrepancies. The fractional release of iodine will be determined and reported later.

3. Of the less volatile fission products, a release of 5.0% of the ^{106}Ru was measured. Although significant releases of fission product silver had been measured in many previous tests, very few useful measurements of this element were obtained in test VI-3. (A small reduction in the resolution of the gamma ray energies in our multichannel analyzer system appears to be the most likely cause of this failure to measure silver.) However, the higher test temperature resulted in significant releases (in the range of 1 to 10% of fuel inventory) of such less volatile species as molybdenum, barium, and uranium.

4. The oxidation behavior of the Zircaloy cladding, as indicated by continuous measurement of hydrogen generation, was in good agreement with a previously developed model, indicating an adequate understanding of this reaction that significantly influences the behavior of some fission products.

5. Measurements of uranium release by three different methods - spark source mass spectrometry, inductively coupled plasma-emission spectrometry, and fluorimetric analysis - indicated that the ICP-ES data compared well with the more precise fluorimetric data. The spark source mass spectrometry results, however, were high by a factor of ~2, which is consistent with the lower precision of this method.

6. Measurements of the masses of deposits collected on the TGTs and the filters verified, as would be expected, that the mass release rates were highest at the maximum test temperature and that the ratio of aerosol to vapor increased with both temperature and time during the test.

7. Posttest examination of the fuel specimen indicated that the cladding was completely oxidized and that only minimal fuel-cladding interaction had occurred. This was additional verification that the planned test conditions had been achieved.

8. The results of this test provided further evidence that the CORSOR-M model is overly conservative. That is, for a range of accident conditions, CORSOR-M predicts higher release rates for the volatile species than are measured for cesium.

7. REFERENCES

1. R. A. Lorenz, J. L. Collins, A. P. Malinauskas, O. L. Kirkland, and R. L. Towns, Fission Product Release from Highly Irradiated LWR Fuel, NUREG/CR-0722 (ORNL/TM-287/R2), Oak Ridge National Laboratory, February 1980.

2. R. A. Lorenz, J. L. Collins, A. P. Malinauskas, M. F. Osborne, and R. L. Towns, Fission Product Release from Highly Irradiated LWR Fuel Heated to 1300–1600°C in Steam, NUREG/CR-1386 (ORNL/TM-346), Oak Ridge National Laboratory, November 1980.

3. R. A. Lorenz, J. L. Collins, M. F. Osborne, R. L. Towns, and A. P. Malinauskas, Fission Product Release from LWR Fuel Under LOCA Conditions, NUREG/CR-1773 (ORNL/TM-388), Oak Ridge National Laboratory, July 1981.

4. R. A. Lorenz, J. L. Collins, and A. P. Malinauskas, "Fission Product Source Terms for the Light Water Reactor Loss-of-Coolant Accident," Nucl. Technol. 46, 404–10 (1979).

5. M. F. Osborne, R. A. Lorenz, J. R. Travis, and C. S. Webster, Data Summary Report for Fission Product Release Test HI-1, NUREG/CR-2928 (ORNL/TM-8500), Oak Ridge National Laboratory, December 1982.

6. M. F. Osborne, R. A. Lorenz, J. R. Travis, C. S. Webster, and K. S. Norwood, Data Summary Report for Fission Product Release Test HI-2, NUREG/CR-3171 (ORNL/TM-8667), Oak Ridge National Laboratory, February 1984.

7. M. F. Osborne, R. A. Lorenz, K. S. Norwood, J. R. Travis, and C. S. Webster, Data Summary Report for Fission Product Release Test HI-3, NUREG/CR-3335 (ORNL/TM-8793), Oak Ridge National Laboratory, March 1984.

8. M. F. Osborne, J. L. Collins, R. A. Lorenz, K. S. Norwood, J. R. Travis, and C. S. Webster, Data Summary Report for Fission Product Release Test HI-4, NUREG/CR-3600 (ORNL/TM-9011), Oak Ridge National Laboratory, June 1984.

9. M. F. Osborne, J. L. Collins, R. A. Lorenz, K. S. Norwood, J. R. Travis, and C. S. Webster, Data Summary Report for Fission Product Release Test HI-5, NUREG/CAR-4037 (ORNL/TM-9437), Oak Ridge National Laboratory, May 1985.

10. M. F. Osborne, J. L. Collins, R. A. Lorenz, K. S. Norwood, J. R. Travis, and C. S. Webster, Data Summary Report for Fission Product Release Test HI-6, NUREG/CR-4043 (ORNL/TM-9443), September 1985.

11. M. F. Osborne, J. L. Collins, R. A. Lorenz, J. R. Travis, C. S. Webster, and T. Yamashita, Data Summary Report for Fission Product Release Test VI-1, NUREG/CR-5339 (ORNL/TM-11104), Oak Ridge National Laboratory, June 1989.

12. M. F. Osborne, J. L. Collins, R. A. Lorenz, J. R. Travis, and C. S. Webster, Data Summary Report for Fission Product Release Test VI-2, NUREG/CR-5340 (ORNL/TM-11105), Oak Ridge National Laboratory, September 1989.

13. R. A. Lorenz, J. L. Collins, and S. R. Manning, Fission Product Release from Simulated LWR Fuel, NUREG/CR-0274 (ORNL/TM-154), Oak Ridge National Laboratory, October 1978.

14. J. L. Collins, M. F. Osborne, R. A. Lorenz, K. S. Norwood, J. R. Travis, and C. S. Webster, Observed Behavior of Cesium, Iodine, and Tellurium in the ORNL Fission Product Release Program, NUREG/CR-3930 (ORNL/TM-9316), Oak Ridge National Laboratory, February 1985.

15. M. F. Osborne, J. L. Collins, P. A. Haas, R. A. Lorenz, J. R. Travis, and C. S. Webster, Design and Final Safety Analysis Report for Vertical Furnace Fission Product Release Apparatus in Hot Cell B, Building 4501, NUREG/CR-4332 (ORNL/TM-9720), Oak Ridge National Laboratory, March 1986.

16. A. G. Croff, ORIGEN2 - A Revised and Updated Version of the Oak Ridge Isotope Generation and Depletion Code, ORNL-5621, Oak Ridge National Laboratory, July 1980.

17. R. A. Lorenz et al., "Prompt Release of Fission Products from Zircaloy-Clad UO_2 Fuels," Sect. 1 in Nuclear Safety Program Annual Progress Report for the Period Ending December 31, 1967, ORNL-4228, Oak Ridge National Laboratory, April 1968.

18. Toshiyuki Yamashita, Steam Oxidation of Zircaloy Cladding in the ORNL Fission Product Release Tests, NUREG/CR-4777 (ORNL/TM-10272), Oak Ridge National Laboratory, March 1988.

19. L. Baker and L. C. Just, "Studies of Metal-Water Reactions at High Temperatures:" III. Experimental and Theoretical Studies of the Zirconium-Water Reaction, ANL-6548, Argonne National Laboratory, 1962.

20. V. F. Urbanic and T. R. Heidrick, J. Nucl. Mater. 75, 251 (1978).

21. M. F. Osborne, J. L. Collins, and R. A. Lorenz, "Experimental Studies of Fission Product Release from Commercial LWR Fuel Under Accident Conditions," Nucl. Technol. 78(2), 157-69 (1987).

22. M. F. Osborne, R. A. Lorenz, J. R. Travis, C. S. Webster, and K. S. Norwood, Data Summary Report for Fission Product Release Test HI-2, NUREG/CR-3171 (ORNL/TM-8667), February 1984.

23. U.S. Nuclear Regulatory Commission, Technical Bases for Estimating Fission Product Behavior During LWR Accidents, NUREG-0772, June 1981.

24. American National Standard Method for Calculating the Fractional Release of Volatile Fission Products from Oxide Fuel, ANSI/ANS-5.4-1982, American Nuclear Society Standards Committee, Working Group ANS-5.4, 1982.

25. M. R. Kuhlman, D. J. Lehmicke, and R. O. Meyer, CORSOR User's Manual, NUREG/CR-4173 (BMI-2122, R3, R4) Battelle Columbus Laboratories, 1985.

NUREG/CR-5480
ORNL/TM-11399
Dist. Category R3

INTERNAL DISTRIBUTION

1. W. S. Aaron
2. C. W. Alexander
3. F. Berrera
4. E. C. Beahm
5. J. T. Bell
6. M. L. Brown
7. D. O. Campbell
8-12. J. L. Collins
13. W. A. Gabbard
14. R. K. Genung
15. P. A. Haas
16. J. R. Hightower
17. E. K. Johnson
18. M. J. Kania
19. T. S. Kress
20-24. R. A. Lorenz
25. J. C. Mailen
26-30. M. F. Osborne
31. G. W. Parker
32. D. J. Pruett
33. C. E. Pugh
34. C. S. Robinson
35. M. G. Stewart
36. R. P. Taleyarkhan
37. J. R. Travis
38. C. S. Webster
39. A. L. Wright
40. A. Zucker
41. Central Research Library
42. ORNL-Y-12 Technical Library Document Reference Section
43-44. Laboratory Records
45. Laboratory Records, ORNL RC
46. ORNL Patent Section

EXTERNAL DISTRIBUTION

47. Office of Assistant Manager for Energy Research and Development, ORO-DOE, P.O. Box 2001, Oak Ridge, TN 37831
48. Director, Division of Reactor Safety Research, U.S. Nuclear Regulatory Commission, Washington, DC 20555
49-50. Office of Scientific and Technical Information, P.O. Box 2001, Oak Ridge, TN 37831
51. Division of Technical Information and Document Control, U.S. Nuclear Regulatory Commission, Washington, DC 20555
52. R. Y. Lee, Accident Evaluation Branch, U.S. Nuclear Regulatory Commission, NLN-353, Washington, DC 20555
53. R. O. Meyer, Accident Evaluation Branch, U.S. Nuclear Regulatory Commission, NLN344, Washington, DC 20555
54. F. Eltawila, Accident Evaluation Branch, U.S. Nuclear Regulatory Commission, NLN344, Washington, DC 20555
55. T. J. Walker, Accident Evaluation Branch, U.S. Nuclear Regulatory Commission, NLN344, Washington, DC 20555
56. K. S. Norwood, 8 Appleford Drive, Abingdon, Oxon OX14, 2DA, United Kingdom
57. S. J. Wisbey, B.220, AERE Harwell, Didcot, Oxon OX11 ORA, United Kingdom
58. T. Yamashita, Nuclear Fuel Chemistry Laboratory, Department of Chemistry, Japan Atomic Energy Research Institute, Tokai-mura, Naka-gun, Ibaraki-ken, 319-11, Japan

59. T. Nakamura, Reactivity Accident Laboratory, Dai-2-Genken-Shinhara-Jutaku-304, 1-23-5, Shinhara, Mito-shi, 310, Japan
60. H. K. Lee, Spent Fuel Storage and Disposal Technology Section, Korea Advanced Energy Research Institute, P.O. Office Box 7, Dae-Danji Choong-Nam, Republic of Korea
61. Y.-C. Tong, Institute of Nuclear Energy Research, P.O. Box 3-6, Lung-Tan, Taiwan, Republic of China

62-311. Given distribution as shown in Category R3 (NTIS - 10)

NRC FORM 335 (2-84) NRCM 1102, 3201, 3202

U.S. NUCLEAR REGULATORY COMMISSION

BIBLIOGRAPHIC DATA SHEET

SEE INSTRUCTIONS ON THE REVERSE

1. REPORT NUMBER (Assigned by TIDC, add Vol No., if any)

NUREG/CR-5480
ORNL/TM-11399

2. TITLE AND SUBTITLE

DATA SUMMARY REPORT FOR FISSION PRODUCT RELEASE TEST VI-3

3. LEAVE BLANK

4. DATE REPORT COMPLETED

MONTH	YEAR
May	1990

5. AUTHOR(S)

M. F. Osborne, R. A. Lorenz, J. L. Collins, J. R. Travis
C. S. Webster, H. K. Lee, T. Nakamura, and Y.-C. Tong

6. DATE REPORT ISSUED

MONTH	YEAR
June	1990

7. PERFORMING ORGANIZATION NAME AND MAILING ADDRESS (Include Zip Code)

Oak Ridge National Laboratory
P. O. Box 2008
Oak Ridge, TN 37831-6285

8. PROJECT/TASK/WORK UNIT NUMBER

9. FIN OR GRANT NUMBER

B0127

10. SPONSORING ORGANIZATION NAME AND MAILING ADDRESS (Include Zip Code)

Division of Systems Research
Office of Nuclear Regulatory Research
U.S. Nuclear Regulatory Commission
Washington, DC 20555

11a. TYPE OF REPORT

Technical

b. PERIOD COVERED (Inclusive dates)

12. SUPPLEMENTARY NOTES

13. ABSTRACT (200 words or less)

Test VI-3, the third in a series of high-temperature fission product release tests in the vertical test apparatus, was conducted in flowing steam. The test specimen was a 15.2-cm-long section of a fuel rod from the BR3 reactor in Belgium, which had been irradiated to a burnup of 42 MWd/kg. Using an induction furnace, it was heated under simulated LWR accident conditions to two test temperatures, 20 min at 2000 K and then 20 min at 2700 K.

The cladding was completely oxidized during the test, and very little melting or fuel-cladding interaction had occurred. Based on fission product inventories measured in the fuel or calculated by ORIGEN2, analyses of test components showed total releases from the fuel of 100% for ^{85}Kr, 5% for ^{106}Ru, 99% for ^{125}Sb, and 99% for both ^{134}Cs and ^{137}Cs. Small release fractions for many other fission products were detected. In addition, very small amounts of fuel material - uranium and plutonium - were released. The total mass released from the furnace to the collection system was 3.17 g, 78% of which was collected on the filters. The results from this test were compared with previous tests in this series and with a commonly used model for fission product release.

14. DOCUMENT ANALYSIS - a. KEYWORDS/DESCRIPTORS

fission product
fission product release
fuel damage

b. IDENTIFIERS/OPEN-ENDED TERMS

15. AVAILABILITY STATEMENT

Unlimited

16. SECURITY CLASSIFICATION

(This page) Unclassified

(This report) Unclassified

17. NUMBER OF PAGES

18. PRICE